Catena 204 (2021) 105377

Contents lists available at ScienceDirect

Catena

journal homepage: www.elsevier.com/locate/catena

Provenance and paleoenvironmental context of the Late Pleistocene thin aeolian silt mantles in southwestern Poland – A widespread parent material for soils

Jaroslaw Waroszewski [a,*], Anna Pietranik [b], Tobias Sprafke [c], Cezary Kabała [a], Manfred Frechen [d], Zdzisław Jary [e], Aleksandra Kot [a], Sumiko Tsukamoto [e], Simon Meyer-Heintze [f], Marcin Krawczyk [e], Beata Łabaz [a], Bernhard Schultz [g], Yulia V. Erban Kochergina [h]

[a] Wroclaw University of Environmental and Life Sciences of Soil Science, Department of Soil Science and Environmental Protection, Grunwaldzka 53, 50-357 Wroclaw, Poland
[b] University of Wroclaw, Institute of Geological Sciences, Borna 9, 50-204 Wroclaw, Poland
[c] University of Bern, Institute of Geography, Hallerstrasse 12, CH-3012 Bern, Switzerland
[d] Leibniz Institute for Applied Geophysics (LIAG), Department of Geochronology, Stillweg 2, 30655 Hannover, Germany
[e] University of Wroclaw, Institute of Geography and Regional Development, 1 Uniwersytecki Sqr, 50-137 Wroclaw, Poland
[f] Institute of Geography and Geology, University of Würzburg, Am Hubland, 97074 Würzburg, Germany
[g] Institut für Mineralogie, Lagerstättenlehre und Petrologie, TU Bergakademie Freiberg, Brennhausgasse 14 09599 Freiberg, Sachsen, Germany
[h] Czech Geological Survey, Geologicka 6, Prague, Czech Republic

ARTICLE INFO

Keywords:
Loess
Cover beds
Strontium and neodymium isotopes
MLA analyses
Geochemistry

ABSTRACT

Thin loess deposits are widespread soil parent materials and important archives for paleoenvironmental reconstruction. The origin of loess in SW Poland is attributed to the Great Odra Valley (GOV), following the general concept that large rivers play a major role in regional silt supply. Yet, the precise provenance (glacier sources and/or local rocks) of silts, possibly deflated from dry GOV braided riverbeds, is not clear. Our study of thin and thick loess mantles in SW Poland for the first time indicates the provenance of thin loess based on mineralogical (MLA-SEM) and isotopic analyses ($^{143}Nd/^{144}Nd$, $^{87}Sr/^{86}Sr$). Luminescence ages of five localities point to thin loess mantle formation during and shortly (23.0 to 17.7 ka yr) after the Last Glacial Maximum (LGM). Our isotopic data indicate that thin loess deposits in SW Poland are the mixtures of two main components – local Sudetic and Scandinavian, the latter delivered by the Fennoscandian ice sheet (FIS). Also, detailed analyses of heavy minerals show that a single mineral (e.g., hornblende) may come from both Sudetic and Scandinavian sources. This research highlights the role of the (Pleistocene) GOV in collecting and homogenizing materials, while supplying the region with fine particles to be deflated by paleowinds from open surfaces. Anomalies in mineralogy and isotopic composition are connected with influence of Sudetic mountain rivers and locally blowing silt material by katabatic winds. Regional grain size differentiation of thin loess mantles explains transport distance and altitude.

1. Introduction

Loess sediments formed mainly by the accumulation of wind-blown silt, cover ca. 10% of the Earth's surface, and are one of the most investigated and best recognized terrestrial sediments (Marković et al., 2008; Antoine et al., 2009; Jary, 2009; Muhs, 2013; Sprafke and Obreht, 2016; Sprafke et al., 2018). Thick loess deposits can provide relatively continuous records of Quaternary paleoenvironmental changes; intercalated paleosols testify to the presence of soil forming processes over millennia (Sprafke, 2016; Zerboni et al., 2014; Schaetzl et al., 2018).

Thin loess deposits (thickness usually <2 m; Schaetzl et al., 2018) have not been as frequently studied as thicker covers, although they are globally recognized, e.g. in Europe (e.g. Kleber and Terhorst, 2013; Boixaidera et al., 2015; Gild et al., 2018; Costantini et al., 2018;

* Corresponding author.
E-mail address: jaroslaw.waroszewski@upwr.edu.pl (J. Waroszewski).

https://doi.org/10.1016/j.catena.2021.105377
Received 7 October 2020; Received in revised form 8 February 2021; Accepted 8 April 2021

Waroszewski et al., 2019), North and South America (e.g. Morrás, 1999; Zárate et al., 2002; Zárate, 2003; Schaetzl and Loope, 2008; Stanley and Schaetzl, 2011; Jacobs et al., 2012; Zárate and Tripaldi, 2012; Luehmann et al., 2013; Schaetzl and Attig, 2013; Schaetzl and Luehmann, 2013; Munroe et al., 2015; Luehmann et al., 2016), Asia (e.g. Lin and Feng, 2015; Yang et al., 2020) and Oceania (e.g. Cattle et al., 2009; Eden and Hammond, 2003; Yates et al., 2018). They often exist at the transition from thick loess to soils and sediments with barely recognizable contributions of aeolian silt (Yaalon and Ganor, 1973; Schaetzl et al., 2018; Waroszewski et al., 2018a; Kowalska et al., 2020). As these deposits are not precisely marked on geological maps they may often be overlooked in the large-scale picture; they might have much stronger imprint in the landscape than previously thought (Lorz and Frühauf, 2013). Knowledge regarding timing and complex studies on thin loess deposition, stratigraphy, spatial distribution and provenance is scarce (e.g., Jacobs et al., 2011; Luehmann et al., 2013; Schaetzl and Attig, 2013; Martignier et al., 2015; Gild et al., 2018; Waroszewski et al., 2020).

Geochemistry and heavy mineral assemblages are powerful tools to estimate the provenance of wind-blown silt (e.g. Újvári et al., 2016a; Ahmad and Chandra, 2013; Muhs et al., 2016; Peng et al., 2016; Muhs et al., 2018; Bosq et al., 2020). While bulk geochemistry is relatively easy to measure, interpretations are problematic in substrates affected by chemical weathering, which is often the case in thin loess deposits. Isotopic provenance tracers independent of chemical weathering (e.g., $^{143}Nd/^{144}Nd$, $^{87}Sr/^{86}Sr$) can inform about the general pattern of provenance but are unable to unravel mixed wind-blown silt sources (Újvári et al., 2016b). Single grain provenance tracers (e.g. zircon, rutile) and their (isotope-)geochemistry and/or U-Pb geochronology track different sediment sources more accurately (Pańczyk et al., 2020; Schatz et al., 2015; Stevens et al., 2010; Újvári et al., 2016b; Újvári and Klötzli, 2015). Furthermore, heavy mineral studies are a promising provenance technique (Chmielowska and Salata, 2020; Peng et al., 2016) that may provide additional important data from sediments and overcome the problems with proper verifying potential sources. Mineral Liberation Analyses (MLA-SEM) is an efficient technique that not only discloses the modal compositions for a large number of heavy mineral grains but also distinguishes multiple populations in a single mineral group. The information includes mineral associations for each mineral, grain size distribution of all heavy minerals as well as semi-quantitative chemical composition (e.g., Pietranik et al. 2018; Tuhý et al., 2020; Przybyło et al., 2020).

Loess in SW Poland mainly dates to the last glacial period, with most prominent silt deposition during Marine Isotope Stage 2 (MIS 2) (Moska et al., 2019; Jary, 1999). For the loess mantle of SW Poland, Badura et al. (2013) suggested that the Great Odra Valley (GOV) was the main source of silt, following the general concept of Smalley et al. (2009) that large, braided rivers play a major role in regional silt supply. Yet, the precise provenance (related to glacier and/or local rocks sources) of silts, possibly deflated from dry GOV riverbeds, is not clear. At present only bulk geochemical data are available from thin and thick loess in SW Poland (Raczyk, 2013; Raczyk et al., 2015 and Waroszewski et al., 2018a, 2019) and they are insufficient to determine its provenance. Complex approaches to loess provenance with at least two independent methods are lacking for SW Poland, whereas recent studies provide first insights into loess origin of eastern Poland based on detrital U-Pb zircon ages (Pańczyk et al., 2020) and a combination of geochemistry and mineralogy (Skurzyński et al., 2020; Chmielewska and Salata, 2020).

This study aims to quantify the proportion of Scandinavian (brought by the Fennoscandian ice sheet (FIS)) and Sudetes silt sources and to clarify the role of the GOV in distributing silt to the loess belt of SW Poland. In addition to thin loess deposits, we sampled thick, loess-paleosol sequences to receive a more complete spatial picture of loess provenance including estimation of proportions from individual sources. Based on field description of 19 sites we chose representative samples for mineralogical (modal proportion between heavy minerals on automated SEM analyses) and bulk isotopic analyses ($^{143}Nd/^{144}Nd$, $^{87}Sr/^{86}Sr$). Grain size data informed us about shifts of modes as a function of transport distance. Additionally, we provide luminescence ages from five sites to assess the timing of silt deposition. The main aims of this multi-method approach are to (1) isotopically characterize thin loess deposits in SW Poland, (2) verify provenance of thin loess deposits regarding their FIS and/or local–Sudetes Mts. sources and (3) link thin loess deposits with the paleoenvironment in which they formed.

2. Study area

The main topographic elements of SW Poland are the Silesian Lowlands and the Sudetes Mountains shared with the Czech Republic in the south (Figs. 1 and 2). The Odra River drains the lowlands from SE to NW, with upstream parts and the main tributaries coming from the Sudetes. The Trzebnickie Hills in the north of the lowlands are moraines that formed during the penultimate (Warta) glaciation (Szczepankiewicz, 1969). To the east the lowlands are limited by the Silesian Highlands (Wyżyna Śląsko-Krakowska).

The Sudetes are divided into two morphological units by the NW-SE trending Sudetic Boundary Fault: (1) a relatively flat Fore-Sudetic Block which is mostly covered by Cenozoic deposits and (2) the Sudetes Mountains. The entire Sudetes area is a complex structural mosaic composed of various types of geological units including: (a) basement units (fragments of Cadomian crustal blocks, variously metamorphosed Palaeozoic sedimentary successions and metaigneous complexes, all stitched by widespread Variscan granitoids), and (b) sedimentary cover, broadly ranging from the Lower Carboniferous (Variscan) to Cenozoic sediments (Kryza and Pin, 2010). The area was affected by Late Cretaceous to Late Pleistocene anorogenic volcanic activity (Birkenmajer et al., 2011).

The FIS maximum advance occurred during MIS 16 (Polish: San 1, NW-European: Cromer C; Marks 2011). During MIS 12 (Polish: San 2; northwest European: Elsterian; Cohen and Gibbard, 2011), the FIS covered almost entirely the Silesian Lowlands (up to 500 m; Hall and Migoń, 2010). The main ice advance during the Saalian (Polish: Odra) is thought to have occurred during MIS 8 or early–middle MIS 6 and covered the Silesian Lowlands and Sudetic Foreland up to an elevation of 300 m asl (Badura and Przybylski, 1998). Finally, area was covered with loess deposits during the last glacial period (Polish: Vistulian; Jary, 2010).

SW Poland is covered with loess and loess derived sediments (Jary 1999, Jary 2010), being a part of European loess belt (Fig. 1). In individual locations, loess thickness reaches 10–15 m as documented in well-studied loess-paleosol sequences e.g., Zaprężyn (Jary and Ciszek, 2004), Biały Kościół (Jary et al., 2004), Księginice Małe (Jary et al., 2001; Chlebowski et al., 2004) or Branice (Jary, 1996). High resolution dating of the thickest loess deposits in SW Poland indicates strong fluctuations in dust accumulation rates during the last glacial period, with peak deposition during MIS2 and minor deposition during MIS3 (Jary, 2007; Jary, 2010; Moska et al., 2019). In general, however, loess deposits in SW Poland occur in scattered patches (medium thickness of 3–5 m) varying in granulometry, geochemistry and stratigraphy (Jary, 2010). Locally, on upland the thickness of these loess mantles may be even reduced to few decimeters (and thus usually unmapped) and mixed with local underlying materials, forming cover beds (Kleber and Terhorst, 2013; Waroszewski et al., 2019). Loess deposits predominate mostly in Fore-Sudetic Block and in the Głubczyce Upland, but are also present in the intrasudetic Kłodzko Basin or to the north of the lowlands (Trzebnickie and Dalkowskie Hills) (Jary, 2010).

The climate in the south-west of Poland is temperate, in the transition from oceanic to continental, with a strong influence of the Sudetes as topographic barrier. Thus, the mean annual precipitation ranges from > 1200 mm in the mountain belt to < 600 mm in the lowlands. Mean annual air temperature oscillates from <2 °C to > 8 °C, respectively (Pawlak, 2008).

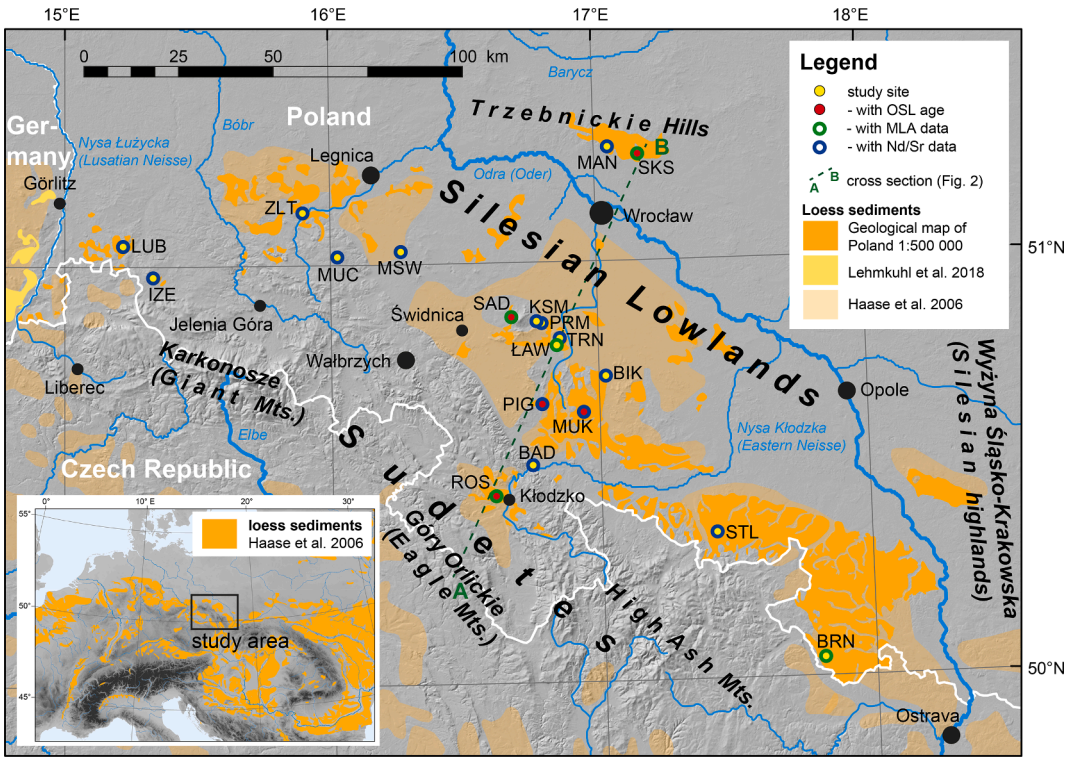

Fig. 1. Location of studied sites in the SW Poland. Loess distribution of Lower Silesia within the European loess belt was formulated based on Geological map of Poland (1:500 000), Lehmkuhl et al., (2018) and Haase et al. (2007) (map of loess sediments in Central Europe adapted from Sprafke 2016, after Haase et al., 2007).

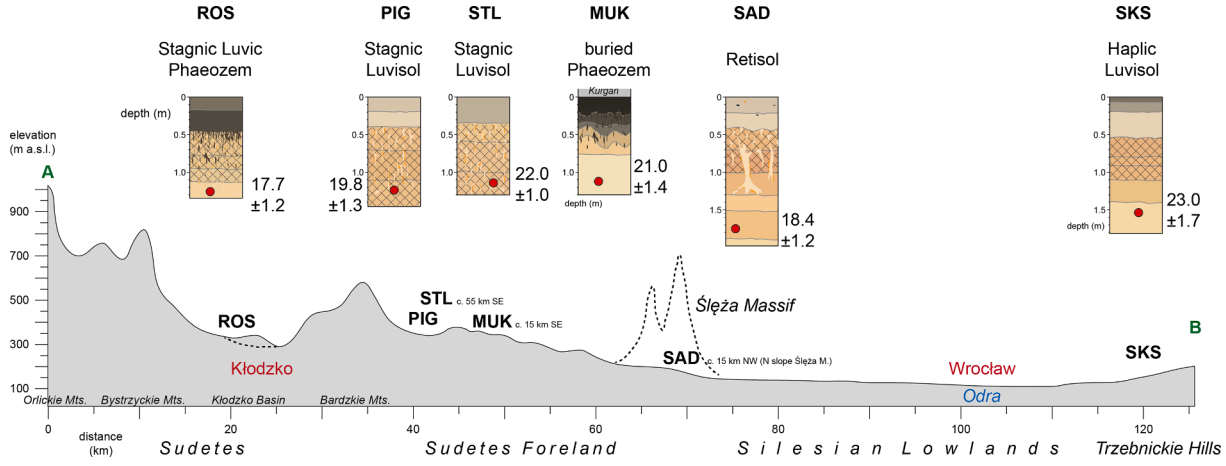

Fig. 2. Cross section tending from S to N showing relief of studied region and position of sites sampled for OSL dating from typical thin loess mantles.

In the south-western Poland, soils developed part of Poland from deep loess deposits or loess derivates exhibit humus-rich topsoils typical for Chernozems and Phaeozems (Labaz et al., 2018; Labaz and Kabala, 2014; Labaz et al., 2019) or consist of subsoil horizons with clay accumulation characteristic of Luvisols (Waroszewski et al., 2018a; Kabala et al., 2015). At the transition from deep loess deposits to areas with their complete absence, the amount of loess/aeolian silt admixture to different underlying materials controls soil evolution and classification (Waroszewski et al., 2018a; 2018b; Waroszewski et al., 2019; Loba et al., 2020). Pure aeolian silt mantles and/or mixed zones may enhance clay translocation and change the direction of soil-forming processes (Waroszewski et al., 2018a).

3. Materials and methods

3.1. Soil sampling

For this study loess samples from 19 sites were collected in south-western Poland from soil profiles, loess-paleosol sequences and archeological sites (Table 1, Fig. 1). Most of the sites represent thin loess deposits (0.2–2.0 m thick) while in case of thick LPS the sampling was limited down to a depth of 2 m below surface. Prior to sampling profiles were cleaned and described following the schemes of sedimentological and pedological standards (FAO, 2006). Soils were classified according to the FAO-WRB system (IUSS Working Group WRB, 2015). Samples for grain-size distribution, mineralogical and isotopic analyses (Table 1) were taken from below modern soils or the lowermost horizon accessible (C or BC, Bt/BC horizons) to reduce as much as possible the influence of

Table 1
Characteristics of sampling sites.

Site	Site acronym*	Coordinates	Altitude (m a.s.l.)	Type of site	Soil horizons	Soil Type (IUSS Working Group WRB, 2015)
Bardo	BAD[b]	N 50°31′5,78″ E 16°44′42,5“	315	soil profile	6BCg	Stagnic Retisol (Siltic, Cutanic)
Biały Kościół[1]	BIK[b]	N 50°43′36.3“ E 17°01’29.9“	190	loess outcrop	C2	Haplic Luvisol (Cutanic, Siltic)
Branice[2]	BRN[a,b]	N 50°2′39.03“ E 17°48’31.34“	315	loess outcrop	C	Stagnic Luvisol (Siltic, Colluvic)
Izery	IZE[b]	N 50°58′40.90“ E 15°19’39.44“	383	soil profile	BC	Stagnic Luvisol (Siltic)
Księginice Małe[3]	KSM[b]	N 50°51′36.3“ E 16°46’11.8“	170	loess outcrop	C2	Stagnic Luvisol (Siltic)
Lubań[4]	LUB[b]	N 51°02′58.7“ E 15°13’10.9“	307	soil profile	BC	Stagnic Retisol (Cutanic)
Łagiewniki	ŁAW[a,b]	N 50°48′7.8“ E 16°50’37.5“	182	soil profile	BC	Luvic Chernozem (Siltic)
Machnice	MAN[b]	N 51°16′15.8“ E 17°03’08.1“	205	soil profile	C1	Stagnic Luvisol (Siltic)
Muchów[5]	MUC[b]	N 51°01′13“ E 16°01’34“	396	soil profile	Btg	Luvic Stagnosol (Siltic)
Muszkowice[6]	MUK[b]	N 50°38′31.0“ E 16°56’21.9“	275	archeological site	Ck	Haplic Pheozem (Siltic)
Mściwojów	MSW[b]	N 51°01′51.5“ E 16°15’54.1“	198	soil profile	Cg	Haplic Chernozem (Siltic)
Piława Górna	PIG[b]	N 50°39′46“ E 16°47’05“	310	soil profile	Btg2	Stagnic Luvisol (Siltic)
Przemiłów[7]	PRM[b]	N 50°51′20.0“ E 16°46’55.3“	225	soil profile	BCg	Stagnic Luvisol (Siltic, Colluvic)
Roszyce	ROS[a,b]	N 50°26′46,66“ E 16°36’21,5“	330	soil profile	Cg	Stagnic Phaeozem (Siltic)
Sady[8]	SAD[a,b]	N 50°52′16.4“ E 16°40’33.2“	248	soil profile	C3	Stagnic Retisol (Siltic, Cutanic)
Skarszyn	SKS[a,b]	N 51°15′09.3“ E 17°09’58.0“	177	soil profile	C	Haplic Luvisol (Cutanic, Siltic)
Stary Las	STL[b]	N 50°20′56.0“ E 17°25’00.5“	294	soil profile	Btg2	Stagnic Luvisol (Siltic)
Trzebnik	TRN[b]	N 50°49′06.9“ E 16°51’20.7“	175	soil profile	Ck	Luvic Chernozem (Pachic, Siltic)
Złotoryja[9]	ZLT[b]	N 51°7′34.09“ E 15°53’48.74“	210	loess outcrop	C2	Stagnic Luvisol (Siltic)

Details regarding morphology of thick loess sequences and thin mantles can be find in: [1]Jary et al., (2004a); [2]Jary (1996); [3]Chlebowski et al., (2004); [4,5] Waroszewski et al., (2019); [6] Kabała et al., (2019); [7,8] Waroszewski et al. (2018a); [9] Kida and Jary (2004);

* Acronyms were use in the text and adopt in selected figures.

[a] Samples selected for MLA analysis.

[b] Samples chosen for Sr/Nd isotopic measurements.

possible pedogenic alterations to a minimum. At the same time, we aimed to not incorporate material from underlying strata of different lithology, which we later could verify based on grain-size and geochemical data (e.g., Luehmann et al., 2013; Waroszewski et al., 2019). Additionally, five samples for luminescence dating were taken from selected layers of profiles arranged in a N-S transect (Fig. 2) to evaluate the age of the thin loess deposits. Steel tubes were hammered into the freshly cleaned outcrop walls of the soil profiles (SKS, MUK, PIG, ROS, STL1). Positions of steel tubes are given in Fig. 2.

3.2. Particle size distribution

A Beckman–Coulter LS 13,320 PIDS laser diffraction at LIAG Hannover measured the particle sizes distribution (PSD) between 0.04 and 2000 μm after dispersion of the samples for 12 h on a rotator using 1% ammonium hydroxide. Laser diffraction has a high spectral resolution (116 classes) and allows the detection of separate modes in PS distribution, which may reflect different sediment sources or a mixing of substrates (Miller and Schaetzl, 2011; Schaetzl and Luehmann, 2013).

3.3. Mineral liberation analyses

The heavy mineral distribution in five selected sites along a N-S transect (SKS, SAD, ŁAW, ROS, BRN; Fig. 1) was identified using the separation technique of Mange and Maurer (1992) and determined in the 0.25–0.06 mm fractions (±fine sand). Heavy minerals were separated using sodium polytungstate solution (2.97 g·cm^{-3}). Most grains obtained from each sample were mounted to glass slides using Canadian balsam and polished to thin sections. Heavy mineral grains were analyzed in five thin sections by mineral liberation analyses (MLA) at the Geometallurgy Laboratory of the TU Bergakademie Freiberg with an FEI Quanta 650F SEM, which was equipped with two Bruker Quantax X-Flash 5030 EDX detectors (analysis conditions: E = 25 kV at spot size = 5.0 μm, beam current = 10nA). A database of minerals was established for the analyzed material by energy dispersive x-ray spectroscopy (EDS) with over 95% phases identified. The data were visualized using MLA Dataview 3.1 software. Heavy minerals were analyzed by automated SEM (MLA) yielding detailed phase information on all grains in the thin sections (SKS n = 1881, ŁAW n = 3103, SAD n = 2878, ROS n = 580 and BRN n = 171). This technique allowed direct identification of both the transparent and opaque minerals as well as the differentiation of simple and complex grains.

3.4. $^{143}Nd/^{144}Nd$ and $^{86}Sr/^{87}Sr$ isotopes

Nineteen loess samples were leached in 2 ml of 2.5 M hydrochloric acid in order to dissolve the carbonate phase. The residual silicate phases were removed by centrifugation and dissolved in the mixture of concentrated HF and HNO_3. Both fractions were dried and then mixed in M HNO_3. Strontium and neodymium fractions were separated by ion-exchange chromatography using AG 50 W-X8 resin (Bio-Rad Laboratories, Inc.); strontium was purified using Sr-spec resin (Triskem Intl.), while LN.spec resin (Triskem Intl.) was used for Nd purification. Strontium and Nd isotopic ratios were analyzed by Thermal Ionization Mass Spectrometry - TIMS Triton Plus (Thermo Fisher Scientific) housed at the Czech Geological Survey. For $^{87}Sr/^{86}Sr$ analysis single Ta filament configuration in static mode was used and mass bias was corrected to $^{88}Sr/^{86}Sr = 8.375209$. For $^{143}Nd/^{144}Nd$ analysis double Re filament configuration in static mode was used and mass bias was corrected to $^{146}Nd/^{144}Nd = 0.7219$. The external reproducibility of Sr and Nd is given by repeat analyses of the JNdi-1 [$^{143}Nd/^{144}Nd = 0.512099 \pm 20$ (2σ, n = 40)] and SRM 987 [$^{87}Sr/^{86}Sr = 0.710252 \pm 36$ (2σ, n = 54)]

3.5. Luminescence dating

Samples for luminescence dating were prepared under subdued red-light condition. The sample material from the outer ~1 cm of both sides of the sampling tubes, which might have been exposed to light, was discarded. The material from the inner part of the tubes was treated with 10% HCl to dissolve carbonates, 3% sodium oxalate to separate aggregates and 30% H_2O_2 to remove organic matter. The fine silt size fraction (4–11 μm) was separated by sedimentation based on Stokes law (Frechen et al., 1995). The prepared polymineral fine grains were settled onto aluminum discs (~2 mg per disc) from a suspension in distilled water. Anomalous fading (Wintle, 1973) of the $pIRIR_{225}$ signal was measured following Auclair et al. (2003) using three aliquots per sample. For all luminescence samples the fading uncorrected ages, obtained by dividing D_e by the dose rate, were corrected using the method of Huntley and Lamothe (2001). Other detailed information about the measurements including applied complete protocol ($pIRIR_{225}$), is

available in Waroszewski et al., (2020).

4. Results

4.1. Morphology and classification of thin loess mantles/soils

Except for studied LPS, the thickness of the investigated loess mantles (Table 1) generally oscillates between 1 and 2 m. Loess mantles were found both on slopes, but also on flat or slightly leveled landforms (e.g., STL, ŁAW, MUK and LUB). Soils at SAD, MSW and PRM sites reveal the presence of colluvium (concave slopes/slope toe) up to 60–90 cm in thickness. Studied thin loess deposits are basically free from coarse fragments except at the PRM, BAD, ŁAW and MUC sites. The first two of them contain two thin intercalations (8–9 cm thick) of sand material, while serpentinite angular gravels were detected in ŁAW and PRM (in BC/C horizons ca.10–20%). At the MUC site, coarse fragments (basalt) are much more abundant compared to other sites, and their content consequently increased from 15% in the topsoil to 30–80% in the subsoil.

Carbonates (Supplementary materials 2) appear in the Ck horizons of the studied thin loess mantles as hard nodules at TRN and MSW sites, while at MUK site carbonates are diffused and sharply separated from overlying non-carbonate soil horizons. Fine–grained secondary carbonates were also noted in the C horizons of Luvisols at KSM, BIK and BRN sites, where content varied from 3.7 to 11.6%. Thin loess mantles in the other sites were completely depleted of carbonates or reveal very small residue in BC horizons (e.g., ŁAW).

Clay translocation and accumulation features are present in the subsoil layers of most of the soils under study, supporting their classification as Luvisols (13 cases). Illuvial horizons (Bt, argic) have strong angular to angular/platy structures with clear clay coatings on soil peds and in biogenic channels. Alternatively, clay accumulation occurs in the form of lamellae (PRM, Table 1). Stagnic properties were recognized in almost all soils with subsoil clay accumulation (Table 1). At MUC these are sufficiently expressed to meet the criteria for a Stagnosol. In all Stagnic Luvisols thin tonging (1–2 cm width and 3–4 cm long) was observed usually below E horizons through Bt horizon until 110–130 cm. However, in four soil profiles (SAD, LUB, IZE, BAD) degradation of argic horizons was observed in the form of large tongues with bleached material breaking argic horizons. These larger tongues were ca. 60–90 cm long and have diameter of 2–5 cm. Large tongues typically create clear polygonal nets (in the horizontal cross-section).

Soils at six sites (Table 1) are characterized with the presence of thick, structural and dark topsoil horizons (A, Ap), fulfilling the criteria for chernic or mollic thus soils were classified as Chernozems or Pheozems. The thickness of A horizons oscillate from 40 to even 90 cm (MSW) in the slope toe position. Disturbances from agriculture (ploughing) were noted only in A horizons till the depth of 25–30 cm.

4.2. Grain-size distribution (GSD)

Almost all samples have a grain size mode in the coarse silt spectrum (Fig. 3, Supplementary materials 2). The most pronounced modes are in the material from thick loess profiles of BIK (40 μm), ŁAW (44 μm), SKS (42 μm), and ZLT (46 μm). Additionally, our grain size (GS) dataset of thin loess deposits reveal a clear spatial pattern in GS mode distribution (Fig. 3). The largest modes (45–46 μm) occur in samples from lowland profiles (e.g., MSC, ŁAW, ZLT, MAN) whereas the smallest modes (28–35 μm) are in profiles at higher topographic positions (e.g. MUC, BRN, ROS). IZE located in the uplands has a GSD comparable to BRN but is bimodal with the main mode at 42 μm and a slightly smaller shoulder peak at 24 μm. MSC is the only profile where sand and silt contents are almost similar, whereas all other profiles are clearly dominated by (coarse) silt. The BC horizons of the loess profiles ŁAW and SKS do not show a clear enrichment in the fine fraction.

4.3. Heavy minerals MLA-SEM

All analyzed grains in presented modal composition (Fig. 4) include simple and complex grains i.e., rock fragments, intergrowths and inclusions in minerals. Heavy mineral composition in all studied localities (SKS, ŁAG, SAD, ROS, BRA) is largely similar, with a predominance of garnet (two types grossular and almandine), hornblende, ilmenite, rutile and Fe-(hydr)oxides. Only the ROS site differs, with a higher abundance of rutile and the absence of Fe-(hydr)oxides. However, all samples feature a high abundance of minor phases (usually each below 5%) and altogether 21 of such minor or very rare phases were detected in all the samples. These phases include a third type of garnet (spessartite-almandine), zircon, tourmaline, muscovite, pyroxene (both diopside and enstatite), Al_2SiO_5 phase (polymorphs not distinguished by MLA), titanite, Ti-magnetite, chlorite and apatite. All mentioned phases occur in all the samples but in diverse proportions (Supplementary materials 1 – Table SM1). For example, SAD site contains twice as much zircon as other sites whereas apatite is absent. SKS is characterized by higher abundance of diopside compared to other sites. ROS has the highest abundance of muscovite and only tracers of pyroxene were detected. BRA has a much higher abundance of titanite and chlorite, but Al_2SiO_5 phases and apatite are absent. Also, at ŁAG site serpentine was detected, which was absent in all other localities.

When different grain sizes are compared among separated fractions,

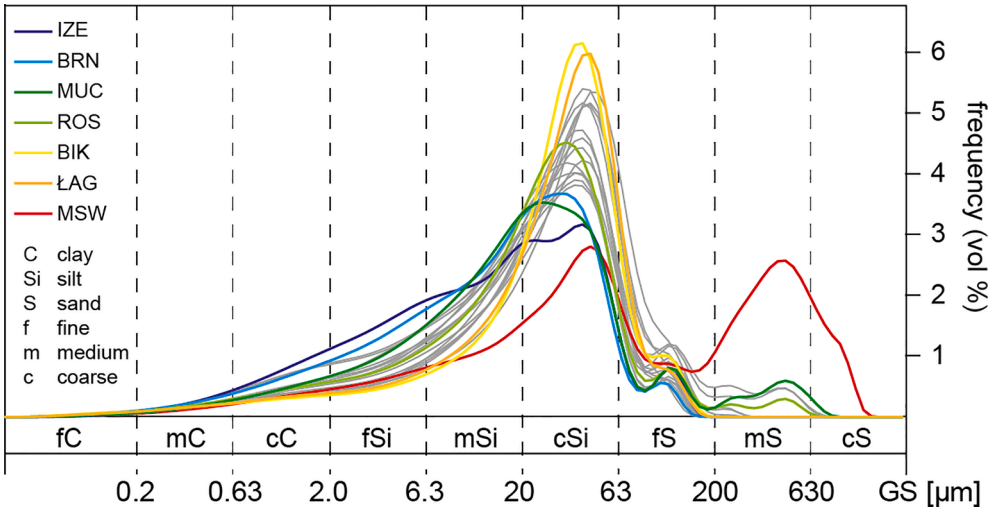

Fig. 3. Grain-size curves for various thin loess mantles illustrating main modes.

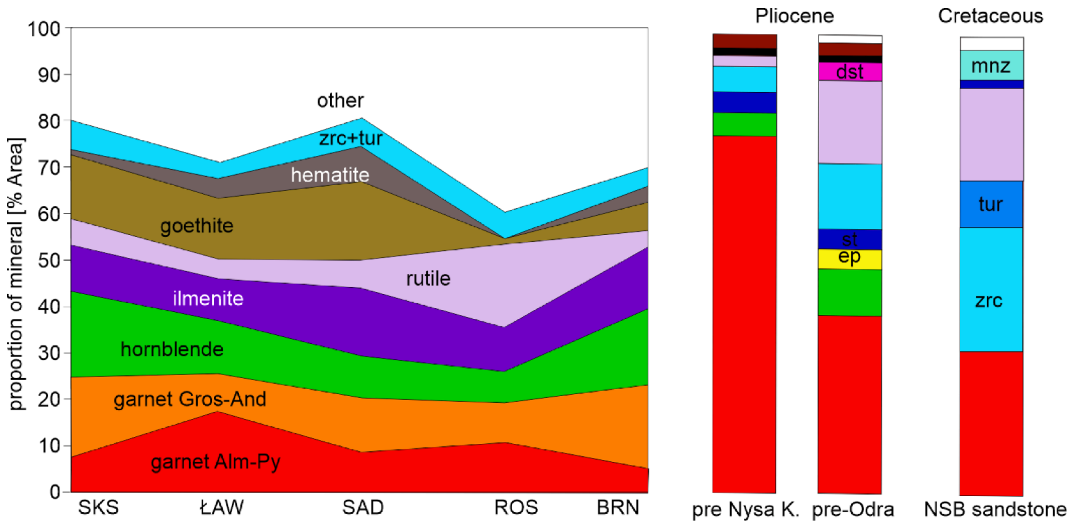

Fig. 4. Modal proportions of heavy minerals at five loess localities compared to heavy mineral assemblage (transparent only) of Pliocene sediments deposited on Fore-Sudetic Block (modified after Zieliński 2018) and that of Cretaceous Jerzmanice sandstones from Sudetes (after Biernacka and Józefiak 2009).

the coarse grain fraction (>150 μm) dominates in SAD (15%), modal proportions are similar between all the grain sizes suggesting generally coarser material deposition in this locality (Supplementary materials – Table SM1). Only 4% of grains belong to the coarse-grained fraction in SKS, the fraction contains predominantly hornblende (>40%), garnets that dominate in the general mode are almost absent. ŁAG also shows predominance of hornblende in the coarser fraction, but the fraction contains also garnets. ROS is characterized by rutile domination in different grain size fractions.

4.4. Sr and Nd isotopes

Sr and Nd isotopes and elemental data were analyzed in nineteen samples (Table 2) and show a relatively limited range of εNd from −11.3 to −13.9 and more variable $^{87}Sr/^{86}Sr$ from 0.7220 to 0.7369. No clear relationships occur between the two isotopic systems (Fig. 5a) and between εNd and Nd contents (Fig. 5b). Two groups can be distinguished in Sr isotopes with ratios below 0.727 in the first group and ratios above 0.730 in the second. The group with lower $^{87}Sr/^{86}Sr$ values has higher Ca and Sr concentrations with the presence of carbonates (Supplementary materials 2) with lower $^{87}Sr/^{86}Sr$ than that in the bulk material (Fig. 5c, d). The major and minor element composition of the samples analyzed for Sr and Nd isotopes is presented in Table SM2 (Supplementary materials 1 and 2).

No clear relationships are observed in the isotopic data by geographic location. The lowest εNd and highest $^{87}Sr/^{86}Sr$ occurs in PIG and one of the highest εNd and lowest $^{87}Sr/^{86}Sr$ in BIK; these two localities are close to each other. Northernmost SKS and MAC localities have similar εNd, but different $^{87}Sr/^{86}Sr$ (Fig. 5a)

4.5. OSL dating

The dose rates are summarized in Table 3. The recycling ratios were within 10% of unity for all measured aliquots and therefore satisfactory. The measured to given dose ratio were all within 10% from unity, indicating that the applied SAR protocol can reliably measure the D_e of samples. The fading rate (g_{2days} value) was between 1.1 ± 0.1 and 1.5 ± 0.1%/decade. The D_e values, fading uncorrected and corrected ages are given in Table 4.

All luminescence ages presented in this study and sampled from the lowermost loess horizons correlate to MIS 2 (Table 3, Fig. 2). They encompass a quite uniform time span, from ca. 17.7 to 23.0 ka (late LGM). The oldest ages (>20 ka) were found at SKS and STL but also in calcareous (secondary carbonate) loess (Ck) in the buried Phaeozem

Table 2
Sr and Nd isotope analyses.

Locality	Horizon/Depth (cm)	$^{87}Sr/^{86}Sr$	2SD	$^{143}Nd/^{144}Nd$	2SD	εNd
BAD	6BCg/102-122	0.733843	0.000011	0.512058	0.000006	−11.3
BIK	C2/180-200	0.721989	0.000016	0.512048	0.000010	−11.5
BRN	C/160-175	0.724856	0.000009	0.512018	0.000010	−12.1
IZE	BC/115-130	0.733410	0.000014	0.512015	0.000006	−12.2
KSM	C2/200-205	0.726463	0.000018	0.511974	0.000007	−13.0
LUB	BC/135-140	0.733502	0.000015	0.511993	0.000008	−12.6
ŁAW	BC/45-61	0.733050	0.000014	0.511955	0.000009	−13.3
MAN	C1/145+	0.734828	0.000009	0.511967	0.000009	−13.1
MUC	Btg/68-83	0.731694	0.000013	0.512029	0.000016	−11.9
MUS	Ck/130-140	0.724493	0.000011	0.511978	0.000007	−12.9
MSW	Cg/110-115	0.735273	0.000012	0.512004	0.000009	−12.4
PIG	Btg2/140	0.736883	0.000016	0.511924	0.000008	−13.9
PRM	BCg/173-200	0.734728	0.000011	0.511940	0.000007	−13.6
ROS	Cg/120-135	0.731818	0.000017	0.511984	0.000010	−12.8
SAD	C3/190+	0.733410	0.000008	0.511981	0.000006	−12.8
SKS	C/145-150	0.725886	0.000010	0.511945	0.000009	−13.5
STL	Btg2/100-125	0.729783	0.000011	0.511999	0.000009	−12.5
TRN	Ck/+120	0.725138	0.000010	0.512009	0.000007	−12.3
ZLT	C2/200	0.733597	0.000010	0.511979	0.000007	−12.9

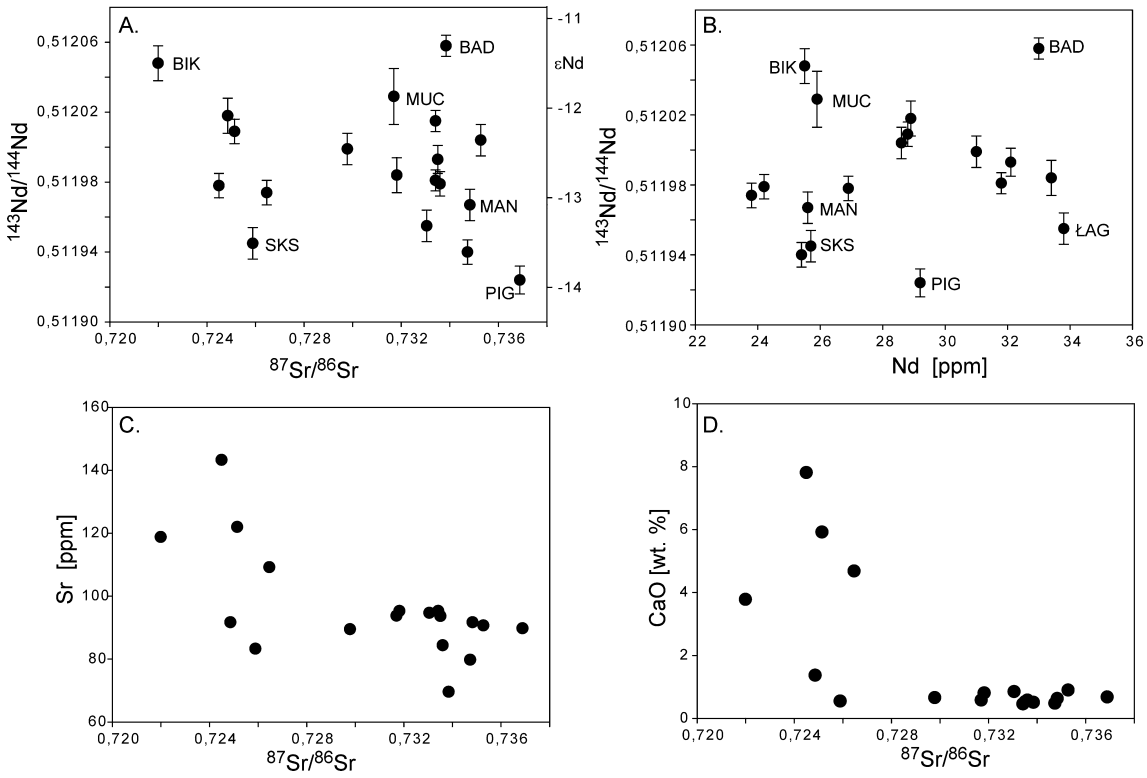

Fig. 5. Sr and Nd isotope composition (a) and their relation to certain elements (b,c,d). Abbreviations for locality names as indicated in Table 1.

Table 3
Radioactivity data and dose rate of selected thin loess mantles.

Sample	Site/horizon	U (ppm)			Th (ppm)			K (%)			Water (%)			Dose rate (Gy/ka)		
LUM3617	MUK/Ck	2,55	±	0,14	9,15	±	0,49	1,73	±	0,10	20	±	10	3,29	±	0,23
LUM3618*	SAD/C3	2,96	±	0,17	10,25	±	0,55	1,83	±	0,10	20	±	10	3,62	±	0,24
LUM3621	ROS/Cg	3,19	±	0,18	11,58	±	0,62	2,00	±	0,11	20	±	10	3,98	±	0,25
LUM3625	SKS/C	2,49	±	0,14	8,52	±	0,46	1,63	±	0,09	20	±	10	3,14	±	0,23
LUM3627	PIG/Btg2	2,89	±	0,01	10,49	±	0,03	1,94	±	0,01	20	±	10	3,73	±	0,23
LUM3628	STL1/Btg2	3,11	±	0,02	11,31	±	0,04	1,91	±	0,01	20	±	10	3,85	±	0,23

* Published in Waroszewski et al., (2020).

Table 4
Equivalent dose, fading rate and ages of selected thin loess mantles.

Sample	Site/horizon	D_e (Gy)			g-value (%/decade)			Fading uncorrected age (ka)			Fading corrected age (ka)		
LUM3617	MUK/Ck	28,5	±	0,1	1,1	±	0,1	19,0	±	1,3	21,0	±	1,4
LUM3618	SAD/C3	59,8	±	0,3	1,2	±	0,1	16,5	±	1,1	18,4	±	1,2
LUM3621	ROS/Cg	63,3	±	0,6	1,2	±	0,2	15,9	±	1,0	17,7	±	1,2
LUM3625	SKS/C	64,7	±	1,1	1,2	±	0,1	20,6	±	1,5	23,0	±	1,7
LUM3627	PIG/Btg2	66,1	±	0,3	1,3	±	0,1	17,7	±	1,1	19,8	±	1,3
LUM3628	STL1/Btg2	73,5	±	0,6	1,5	±	0,1	19,0	±	1,2	22,0	±	1,0

(MUK). The younger ages were obtained in thin loess from ROS, PIG and SAD sites.

5. Discussion

5.1. Loess sources in SW Poland – Views for the provenance

For many decades, the origins of wind-blown silt in SW Poland were attributed for many decades to glaciers being most efficient in producing silt (Jahn, 1950). However, during the last glacial, only the highest peaks of the Sudetes were glaciated (Hall and Migoń, 2010). During the penultimate glaciation, the Fennoscandian ice sheet (FIS) ended north of Wroclaw, but it did not reach SW Poland during the last glaciation (Hall and Migoń, 2010). The southernmost last glacial FIS ice marginal valley was c. 50 km north of the Odra Valley region that served as northwest flowing ice marginal valley during the penultimate glacial (Badura et al. 2013). Next to glaciers, also frost weathering may produce silt, therefore the Sudetes drained by Odra and it's tributaries may provide local sources of silt to the loess belt of SW Poland.

Jary and Kida (2000) considered marginal and proglacial zones as the main source of fine particles blown out of the foreground of the FIS. This view has been revised by Badura et al., (2013), who suggest the presence of the GOV that served as ice marginal valley during the penultimate glacial. The Sudetes drained by Odra (major river) and its tributaries flowing from the mountains may provide local sources of silt. Together with silt derived from FIS sources fine-grained material was

subsequently deflated and transported to the south and SE and formed the loess belt of SW Poland. Badura et al, (2013) postulate that significant proportion of ice sheet derived silt can only be detected in MIS4–MIS2 loess, whereas older loess deposits are related to supply by GOV from the Sudetes. Until now, differentiation of proportions of silt coming from FIS and Sudetic sources has remained unknown.

5.2. Differentiating FIS vs. Sudetic provenance of wind-blown silt in SW Poland

Chemical composition of loess is generally, but not always, similar worldwide and approaches the isotopic composition of the upper continental crust (Gallet et al. 1996, Chauvel et al. 2014). The differences in certain elements and isotopes may appear due to the proportions of heavy minerals (from depositional and loess recycling processes) that control concentrations of these elements e.g., Zr and Hf in zircon, light rare earth elements (LREE) in monazite, heavy rare earth elements (HREE) in garnet and Ti in ilmenite and titanite (e.g., Chauvel et al. 2014). Sr isotopes can also be fractionated by grain sorting in relation to transporting medium (Tütken et al., 2002). Generally, isotopes record the averaged source composition (Gallet et al. 1996; Muhs et al., 2018), while heavy minerals may record and track input from multiple sources (Morton and Hallsworth 1999, Marcinkowski and Mycielska-Dowigałło, 2013, Zieliński 2018, Chmielowska and Salata 2020).

5.2.1. Nd and Sr isotopes

Comparison of isotopic composition of the studied thin loess deposits with possible source areas shows none of the rocks in the Sudetes and Fore-Sudetic Block has as low εNd as the studied loess (Fig. 6, Table 2). The lowest ratios were reported for gneisses from Śnieżnik and Gierałtów (from −2.4 to −9.1, Lange et al., 2005a) and Izera Mts. (from −5.0 to −10.6, Oberc-Dziedzic et al., 2005), while similar εNd (from −8.9 to −11.2) was measured in Triassic sandstones derived from Sudetic lithologies (Konieczna et al., 2015). Also, gneisses and granulites from Sowie Mountains have higher εNd, the lowest one is in granulites from −8.0 to −11.5 with a single sample with εNd = −15.9 (O'Brien et al., 1997). Usually $^{87}Sr/^{86}Sr$ ratios are also lower in Sudetic and Fore-Sudetic rocks compared to loess, although strong post-Variscan alteration resulting in a very high $^{87}Sr/^{86}Sr$ ratios was observed e.g., in Śnieżnik and Gierałtów gneisses (Lange et al., 2005a). However, other localities including Góry Sowie gneisses with present day $^{87}Sr/^{86}Sr$ from 0.711to 0.722 (Bröcker et al. 1998) do not show such alteration. On the other hand, crystalline rocks from Scandinavia have lower εNd and seemingly also higher $^{87}Sr/^{86}Sr$ than the thin loess samples in this study (Valbracht et al., 1994; Appelquist et al. 2011, Rutanen et al., 2011; Johansson et al., 2016). Interestingly, the variability observed in the isotopic composition of the studied material in notably low. Therefore, we suggest that the observed isotopic composition is consistent with the following:

(1) Loess material was well homogenized, probably during fluvial/aeolian transport and deposition, thus the particular regional sources (predominately FIS or predominately Sudetic) cannot be distinguished between the studied localities
(2) Loess material is a mixture of two components Sudetic and FIS and geochemical modelling implies that 30–50% of FIS material is mixed with that derived from local mountains (Fig. 6).
(3) Lower $^{87}Sr/^{86}Sr$ ratios in samples containing carbonates may suggest that this particular material was sourced from Sudetic region.

The analyses show that εNd and $^{87}Sr/^{86}Sr$ isotopic composition of the loess correspond to those of Late Quaternary ice-proximal sediments (Farmer et al. 2003) as well as those deposited in Małopolska terrains from Middle Cambrian to Silurian (Walczak and Belka, 2017). Both sedimentary units (Quaternary and Paleozoic) exhibit mixed provenance of material originating from both younger Avalonian and Cadomian sources (dominating in Sudetes) and older Baltica-derived ones (dominating in Scandinavia, Walczak and Belka, 2017).

5.2.2. Heavy minerals record

Heavy minerals are often used to reconstruct the source of aeolian material and wind directions (Römer et al. 2016, Wolf et al. 2019). The main challenge to distinguish Sudetic from Scandinavian sources in the

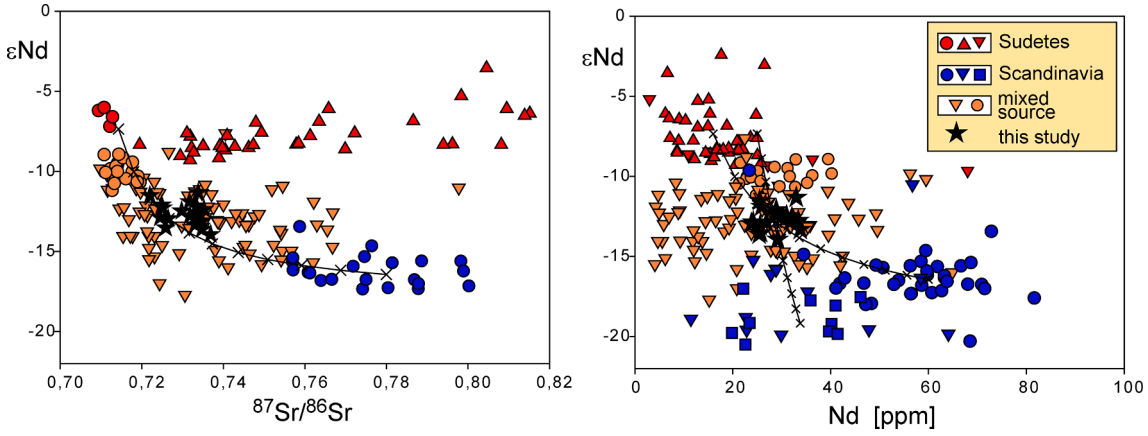

Fig. 6. Comparison of Nd and Sr isotopic composition and Nd content in loesses to chosen crystalline and sedimentary rocks from Sudetes and Scandinavia as well as presumed mixtures of both sources (Other). Data from Sudetes are from: Gęsiniec Variscan intrusion (red circles, Pietranik et al., 2018), Śnieżnik and Gierałtów gneisses (red traingles - Lange et al., 2005b), Izera gneisses (red upturn triangles - Oberc-Dziedzic et al. 2005). Data from Scandinavia are: Bornholm granitoids (blue circles – Johansson et al. 2016), granitoids from central Sweden (blue squares – Appelquist et al. 2011), Bergslagen granites (blue upturn triangles - Valbracht et al. 1994). Other data include Triassic sandstones deposited in Silesia (orange circles – Konieczna et al., 2015 – dominating provenance Sudetic) and Cambrian to Sylurian clastic rocks of Małopolska and Łysogóry terrains (Walczak and Belka, 2017) – mixed Baltica – Gondwana provenance). All data are present-day values. Solid lines are probable models of mixing between Sudetic and Scandinavian sources, end–members are taken as average Sudetic composition for Nd isotopes and Nd content and average Sr isotope composition for unaltered Sudetic rocks (SUDETIC end memeber) and average Bornholm composition (SCANDINAVIAN end member). If average of Swedish granites is taken instead (SCANDINAVIAN end member) the Nd content in Sudetic component has to be at its highest, however generally higher Nd content in sediments derived from Sudetes as compared to crystalline rocks suggests that it is also a probable approach. Regardless of the approach the proportion of Sudetic end–member in studied loess deposits is 50–70% (as indicated by crosses on the model spaced at 10%). (For interpretation of the references to colour in this figure legend, the reader is referred to the web version of this article.)

studied thin loess. This is because Sudetic crystalline rocks may provide similar mineral assemblages compared to glacial, freshly eroded material from a Scandinavian source (Zieliński 2018). The Pliocene fluvial sediments from rivers draining the Sudetes and the Fore-Sudetic Block (Badura and Przybylski, 2004), the Quaternary glacial deposits from Central Poland (Marcinkowski and Mycielska-Dowigałło, 2013; Weckwerth and Chabowski, 2013) and the loess samples analyzed in this study, have similar assemblages of major heavy minerals (Fig. 4). Dominating transparent minerals i.e., garnet, hornblende, rutile, zircon and turmaline are present in high proportions in all of the mentioned sediments and the main difference is the absence of staurolite and epidote in thin loess deposits, albeit these minerals never were dominating ones. Similar minerals were also observed in loesses from Tatra Mountains with the source correlated with pre-Variscan basement cropping out in the mountains in essence similar to that occurring in Sudetes (Chmielowska and Salata 2020). Analyses of only modal proportion of heavy minerals often do not provide unambiguous information on provenance in complex areas. However, the information on heavy minerals is not only modal, because sometimes one mineral group may contain chemically variable components coming from different source rocks. Garnet, as an example, can hold numerous chemical varieties depending on the rock type and locality in Sudetes (Biernacka and Józefiak 2009). Hornblende (Fig. 7) is another prime example as it may be common in both Sudetes and Fennoscandian rocks (Zieliński 2018). Due to its low preservation in sediment it is probable that it was derived from crystalline rocks and was not redeposited. Largest hornblende grains occur in the northernmost studied site SKS suggesting Scandinavian origin, however, at least three, structurally different types of hornblende can be distinguished (Fig. 7). For example, smallest hornblende grains are associated with grossular garnet and occur in all the loess localities, but the largest grains of this association are observed to the south suggesting local contribution (Fig. 8). Therefore, we interpret

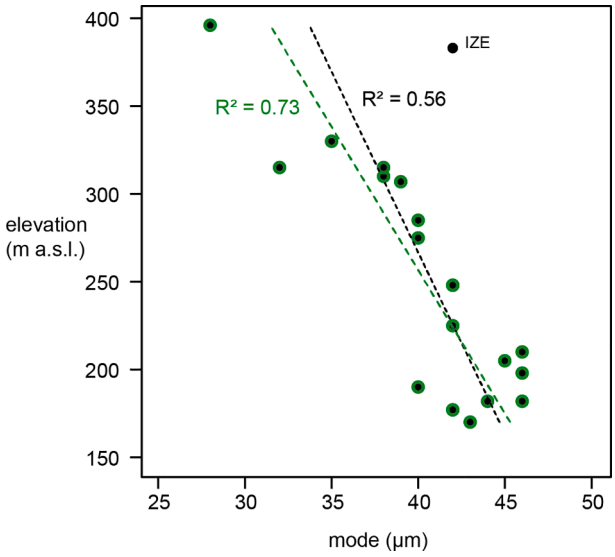

Fig. 8. Relationship between an altitude and grain size mode of studied loess mantles (Pearson correlation).

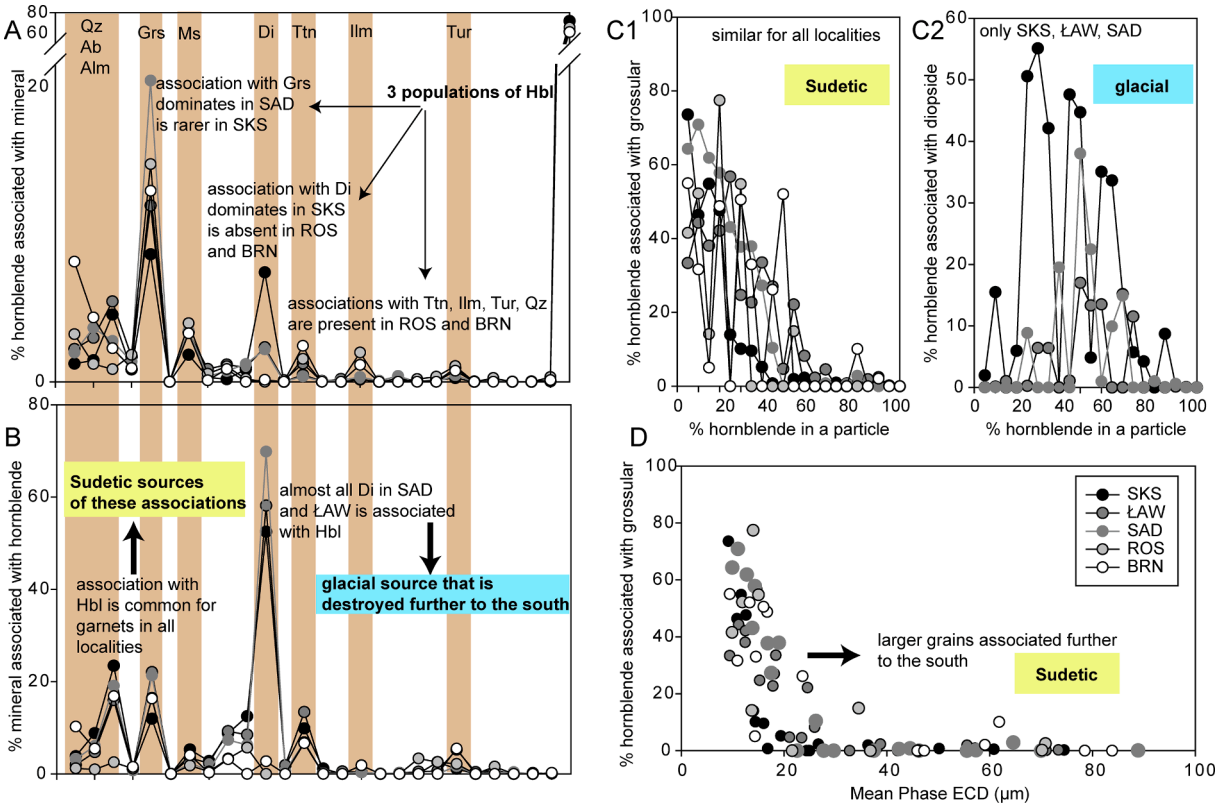

Fig. 7. Data from automated MLA-SEM, all proportions in % area (a) proportion of hornblende associated with different minerals shown for all analyzed localities, the last symbol on x-axis represents proportion of liberated hornblende i.e. not associated with any mineral, three groups are indicated based on different hornblende+other minerals assemblage (b) proportion of each mineral that is associated with hornblende in each locality, brownish vertical columns for a and b identify the same mineral in both plots (mineral abbreviations after Kretz, 1983), (c) proportion of hornblende in assemblages with grossular (c1 –grains containing more hornblende have less grossular) and diopside (c2 – grains contain similar proportions of hornblende and diopside within grain) – differences are interpreted as different sources of the two assemblages, (d) grains size of hornblende in grossular+hornblende associations (expressed as mean Equivalent Circle Diameter – please note that size distribution is similar between localities, although the largest grains with low grossular content seem to dominate in BRN and SAD.

this association as sourced from the Sudetes. Depending on the locality, 10% to 20% of hornblende belongs to this group. Another type of hornblende, associated with diopside, enstatite and sometimes spessartine garnet occurs in SKS, SAD and ŁAG. However, diopside association dominates in SKS, whereas enstatite one in SAD and ŁAG. Considering that fresh diopside + hornblende rock is not a common lithology in the Sudetes, but it dominates in the northernmost SKS locality it may indicate its origin from Fennoscandia cumulates. Also, diopside grains are the largest in SKS as expected if they were derived from the glacial source. Yet another source for hornblende is suggested for ROS and BRA, where this mineral is associated with accessory phases such as ilmenite, titanite and tourmaline. Therefore, hornblende can be related to different sources both identified as Sudetic and as Scandinavian lithologies (Table 5) consistent with isotopic data. Analyses of other heavy mineral phases draw similar implications (See Supplementary Material 1).

5.3. Chronology and paleoenviroment – Implications for silt transport and reevaluation of provenance model

LPS in SW Poland record Late Pleistocene loess deposition, with peak silt accumulation dated to MIS 2 (Jary, 1999), e.g., 20–25 ka at Bialy Kościół (herein: BIK). Our luminescence ages from six thin loess sites (SAD dated by Waroszewski et al., 2020) group around 17–23 ka. All samples from sediments and deep soil horizons without clear signs of bioturbation, which is underlined by the quite narrow scatter of luminescence ages. Luminescence ages in cover beds on the Swiss Plateau yielded similar single grain and luminescence ages, indicating that mixing did not alter the sediment ages in several decimeters' depth (Veit et al. 2017). Waroszewski et al. (2020) demonstrated that at SAD and nearby loess mantles of only few decimeters thickness still yield Late Pleistocene ages (11–14 ka), which is surprising in the presence of treefall and zooturbation. Ages in this time range and stratigraphic position correspond to upper periglacial cover beds according to Kleber et al. 2013), whereas lower loess dominated cover beds are termed intermediate layers. The ages of the Intermediate layers in the Bavarian forest reach up to 23.5 ka (Huber, 2014) or 25.5 ka (Völkel and Mahr 1997). In the Vienna Forest (NE Austria), Frank et al. (2011) dated reworked loess attributed to intermediate layers to 20–30 ka. In the Taunus Mountains (Germany), Hülle et al. (2009) reported ages of 19–23 ka. Döhler et al. (2018) obtained three ages from reworked loess between intermediate layers in the range of 21–25 ka.

Clark et al. (2009) defined the period between 26 and 19 ka as the global LGM. In the Alps the maximum ice advance occurred around 24–25 ka (Seguinot et al. 2018), whereas the maximum last glacial FIS advance to Germany may have occurred already during late MIS 3 (Hardt et al. 2016). From NW Germany to E Germany to SW Poland, there appears a large gap between the last glacial FIS and the loess belt close to the Central European Highlands. Probably last glacial FIS ice-marginal valleys were less relevant silt sources compared to large rivers further south, e.g. the GOV and their tributaries (Badura et al. 2013). However, our provenance data, clearly indicate a strong FIS contribution to loess in SW Poland. We thus assume that erosion of older glacial and glacifluvial sediments and recycling of loess deposits (Van Loon, 2006) are important last glacial silt sources.

For the southwestern Poland, based on the available framework we can reconstruct a large periglacial river landscape in the Silesian lowlands that was drained by the braided Odra River. Sediments collected by its tributaries are both, resulting both from frost weathering (Sudetes) and recycling of mid-Pleistocene deposits (likely with predominant FIS components). From the mixed material GOV floodplains material was deflated to the surrounding areas by westerly to northwesterly winds, creating a geographically broad drape of aeolian silt. Appearance of local isotopic and mineralogical anomalies (e.g., BAD) suggest importance of smaller mountain rivers e.g., Nysa Kłodzka in local supply with wind-blown silt. Therefore, Odra and it's tributaries provide homogenous fine-grained material close to the GOV, while in Sudetes locally blowing out silt, via katabatic winds, decide on the existence of some differences between loess mantles.

Our grain size distribution data indicates that coarse loess dominates in the lowlands, whereas in the uplands to the south, grain sizes become finer. This relation is reflected by the GS mode that decreases from ≥ 40 μm at sites lower than 300 m a.s.l. to < 40 μm at sites above 300 m a.s.l. A single exception is IZE, with a twin peak at 42 μm (larger) and 24 μm (smaller). Twin peaks in loess samples reported first by Machalett et al. (2008) for the loess profile Remizovka (Kazakhstan) are likely an artefact of Beckman Coulter particle sizers (Schulte et al. 2018) and may be related to a specific mineralogical composition. Therefore, we assume that the GS mode at IZE is lower than measured herein. When excluding IZE (Fig. 8) there is a clear relationship of altitude (m a.s.l.) and mode (μm), with $R^2 = 0.73$ (0.56 with IZE included). Median ($R^2 = 0.54$) is less clear in demonstrating this relation, as this parameter is more sensitive to coarse and fine GS admixtures. Several profiles have small secondary modes in the sand size that are related to coarse material admixture by reworking of loess along slopes that does not seem to affect the main mode in GSD (Fig. 3). In Bt horizons this coarse mode likely relates to the formation of Mn-Fe nodules due to redoximorphic conditions in the horizons enriched in clay due to its down-profile translocation (e.g., Waroszewski et al., 2019). We further note a slight increase in fine fractions (clay and fine silt) in the Bt and BC horizons of soils in thin aeolian silts, which are due to weathering, but again, do not affect the main GS mode.

The comparably small influence of weathering/pedogenesis and local admixtures to grain sizes modes suggest that regional grain-size variations highlight mostly past sedimentary dynamics. The spatial pattern of silt modes indicates the influence of transport distance and altitude dependent sorting (Pye, 1995). Instead of local deflation centers, we can infer a predominant fluvial transport of silt (and other grain sizes) to the GOV, where silt is deflated from dry riverbeds to the surroundings. This involves aeolian transport of silt to the erosion / production areas, including a gradual fining with altitude (Pye, 1995). A comparable model was developed for the Tien Shan foothills in Central Asia, where silt produced in the mountains is washed to the lowland deserts, deflated, and transported by wind to the foothills of the mountain range (Machalett et al 2006). These paleowinds might be related to prevailing northwesterly wind in central and eastern Europe during Late Pleniglacial (MIS 2; Bokhorst et al., 2011) but also katabatic

Table 5
Possible sources among described mineral phases.

Mineral	Description	Suggested source
Garnet Grossular-Almandine	2 types: (1) Associated with hornblende (large in SAD) and (2) fully liberated (large in SKS)	Mixed: (1) amphibolite from Sudetes, (2) glacial
Garnet Almandine-Pyrope	Diverse associations, ROS much different to the other localities	Sudetic: felsic gneisses, mafic granulites and/or redeposited Mezozoic to Cenozoic sediments
Hornblende	Diverse associations, ROS and BRN much different grains from SKS, ŁAW and SAD	Mixed: Sudetic and glacial, glacial dominates in SKS
Ilmenite	Diverse associations, BRN different	Several sources, local for BRN
Rutile	Very uniform associated with felsic minerals	Metamorphic rock, common for all localities, perhaps redeposited glacial or Sudetic source
Zircon	Scarce, different types of grains for ŁAW and SAD	Some zircon from local sources
Turmaline	Different groups identified for (1) SKS, ŁAW and SAD, (2) BRN and (3) ROS	Numerous sources
Hematite and Goethite	Dominates in ŁAW and SAD, occurs in SKS	Secondary mineral, suggesting redeposition from older loesses

winds from the FIS responsible for more direct transport of fine particles into the Sudetes foothills and mountain valleys. Badura et al., (2013) confirmed that during MIS 2 blowing of silt size material occurred in south and SE direction (finer material).

6. Conclusions

Our study provides a view on the provenance of thin loess deposits in SW Poland with yet unmatched detail. Luminescence ages indicate that thin loess deposits representing mostly upper and intermediate periglacial cover beds are slightly younger than peak loess accumulation in the SW Poland. Applied isotopes ($^{143}Nd/^{144}Nd$, $^{87}Sr/^{86}Sr$) and mineralogy (MLA-SM) helped to identify loess sources but also define their proportions. Both isotopic and mineralogical tools point out to mixed (Sudetic and Scandinavian) provenance of almost all thin loess deposits. εNd and $^{87}Sr/^{86}Sr$ values suggest Avalonian/Cadomian and Baltica sources of wind-blown silt. Geochemical modelling estimates very similar proportions of FIS material and local Sudetic substrate. This highlights the role of the GOV in strongly homogenizing both geochemical and mineralogical signals, in reworking fine particles, as well as in supplying whole region with wind-blown dust during MIS 2. Furthermore, thin loess mantles become progressively finer with higher altitudes and larger distance from the GOV, which indicates its role as main deflation center. Our data underline that the GS mode is most illustrative to quantify this gradual fining, as it is to a certain extent independent of coarse material admixture by slope processes and fine material development from in-situ weathering.

CRediT authorship contribution statement

Jaroslaw Waroszewski: Conceptualization, Methodology, Writing - original draft & Editing, Project administration, Funding acquisition. **Anna Pietranik:** Formal analysis, Writing - review & editing, Visualisation. **Tobias Sprafke:** Formal analysis, Visualisation, Writing - review & editing. **Cezary Kabała:** Writing - review & editing. **Manfred Frechen:** Methodology, Writing - review & editing. **Zdzisław Jary:** Writing - review & editing. **Aleksandra Kot:** Writing - review & editing. **Sumiko Tsukamoto:** Methodology, Writing - review & editing. **Simon Meyer-Heintze:** Data curation, Writing - review & editing. **Marcin Krawczyk:** Writing - review & editing. **Beata Łabaz:** Writing - review & editing. **Bernhard Schultz:** Formal analysis, Writing - review & editing. **Yulia V. Erban Kochergina:** Formal analysis, Writing - review & editing.

Declaration of Competing Interest

The authors declare that they have no known competing financial interests or personal relationships that could have appeared to influence the work reported in this paper.

Acknowledgements

This research was financed by National Science Center (Poland) projects Sonata 8 No 2014/15/D/ST10/04087 (awarded to Jaroslaw Waroszewski), Opus 15 No 2018/29/B/ST10/01282 (awarded to Jaroslaw Waroszewski) and No 2018/29/B/ST10/00610 (awarded to Beata Łabaz), NAWA PROM programme grant No PPI/PRO/2018/1/00004/U/001 (awarded to Tobias Sprafke) as well as Leading Research Groups support project from the subsidy increased for the period 2020–2025 in the amount of 2% of the subsidy referred to Art. 387 (3) of the Law of 20 July 2018 on Higher Education and Science, obtained in 2019. Authors are grateful to Elżbieta Musztyfaga for technical preparation of luminescence samples. We thank also two anonymous reviewers who helped to improve the final version of the manuscript.

Appendix A. Supplementary material

Supplementary data to this article can be found online at https://doi.org/10.1016/j.catena.2021.105377.

References

Ahmad, I., Chandra, R., 2013. Geochemistry of loess-paleosol sediments of Kashmir Valley, India: provenance and weathering. J. Asian Earth Sci. 66, 73–89.
Antoine, P., Roussea, D.D., Moine, O., Kunesch, S., Hatté, C., Lang, A., Tissoux, H., Zoller, L., 2009. Rapid and cyclic aeolian deposition during the last glacial in European loess: a high-resolution record from Nussloch Germany. Quaternary Sci. Rev. 28 (25–26), 2955–2973.
Appelquist, K., Brander, L., Johansson, Å., Andersson, U.B., Cornell, D., 2011. Character and origin of variably deformed granitoids in central southern Sweden: implications from geochemistry and Nd isotopes. Geol. J. 46, 597–618.
Auclair, M., Lamothe, M., Huot, S., 2003. Measurement of anomalous fading for feldspar IRSL using SAR. Radiat. Meas. 37, 487–492.
Badura, J., Przybylski, B., 1998. Extent of the Pleistocene ice sheets and deglaciation between the Sudeten and the Silesian Rampart. Biuletyn Instytutu Geologicznego 385, 9–28 (In Polish with English summary).
Badura, J., Przybylski, B., 2004. Evolution of the Late Neogene and Eopleistocene fluvial system in the foreland of the Sudetes Mountains, SW Poland. Annates Soc. Geologomm Pol. 74, 43–61.
Badura, J., Jary, Z., Smalley, I., 2013. Sources of loess material for deposits in Poland and part of Central Europe: the lost Big River. Quat. Int. 296, 15–22.
Biernacka, J., Józefiak, M., 2009. The eastern sudetic Island in the early-to-middle Turonian: evidence from heavy minerals in the Jerzmanice sandstones, SW Poland. Acta Geol. Pol. 59, 545–565.
Bokhorst, M.P., Vandenberghe, J., Sümegi, P., Łanczont, M., Gerasimienko, N.P., Matviishina, Z.N., Marković, B., Frechen, M., 2011. Atmospheric circulation patterns in central and eastern Europe during the Weichselian Pleniglacial inferred from loess grain-size records. Quaternary Int. 234 (1–2), 62–74.
Bosq, M., Bertran, P., Degeai, J.-P., Queffelec, A., Moine, O., 2020. Geochemical signature of sources, recycling and weathering in the Last Glacial loess from the Rhône Valley (southeast France) and comparison with other European regions. Aeolian Res. 42.
Birkenmajer, K., Pécskay, Z., Grabowski, J., Lorenc, M.W., Zagożdżon, P., 2011. Radiometric dating of the Tertiary volcanics in lower Silesia, Poland. VI.K-Ar and paleomagnetic data from basaltic rocks of the West Sudety mountains and their northern foreland. Ann. Soc. Geol. Pol. 81, 115–131.
Boixadera, J., Poch, R.M., Lowick, S.E., Balasch, C., 2015. Loess and soils in the eastern Ebro Basin. Quat. Int. 376, 114–133.
Bröcker, M., Żelaźniewicz, A., Enders, M., 1998. Rb–Sr and U-Pb geochronology of migmatitic gneisses from the Góry Sowie (West Sudetes, Poland): the importance of Mid-Late Devonian metamorphism. J. Geol. Soc. 155, 1025–1036.
Cattle, S.R., Greene, R.S.B., McPherson, A.A., 2009. The role of climate and local regolith-landscape processes in determining the pedological characteristics of aeolian dust deposits across south-eastern Australia. Quat. Int. 209, 95–106.
Chauvel, C., Garçon, M., Bureau, S., Besnault, A., Jahn, B.M., Ding, Z., 2014. Constraints from loess on the Hf–Nd isotopic composition of the upper continental crust. Earth Planet. Sci. Lett. 388, 48–58.
Chlebowski, R., Ciszek D., Jary Z., Kida J., 2004. Origin of loess from Księginice Małe (Śleża Massif) based on heavy minerals analysis. W: Polskie Towarzystwo Mineralogiczne – Prace Specjalne, 24, Uniwersytet Śląski, 115–118.
Chmielowska, D., Salata, D., 2020. Heavy minerals as indicators of the source and stratigraphic position of the loess-like deposits in the orava basin (polish Western Carpathians). Minerals 10, 445.
Clark, P.U., Dyke, A.S., Shakun, J.D., Carlson, A.E., Clark, J., Wohlfarth, B., Mitrovica, J. X., Hostetler, S.W., McCabe, A.M., 2009. The last Glacial Maximum. Science 325, 710e714.
Cohen, K.M., Gibbard, P.L., 2011. Global chronostratigraphical correlation table for the last 2.7 million years (chart + documentation). Subcommission on Quaternary Stratigraphy (International Commission on Stratigraphy), Cambridge.
Costantini, E.A.C., Carnicelli, S., Sauer, D., Priori, S., Andreetta, A., Kadereit, A., Lorenzetti, R., 2018. Loess in Italy: genesis, characteristics and occurrence. Catena 168, 14–33.
Eden, D.N., Hammond, A.P., 2003. Dust accumulation in the New Zealand region since the last glacial maximum. Quat. Sci. Rev. 22, 2037–2052.
FAO, 2006. Guidelines for Soil Description. 4rd Ed. FAO, Rome.
Farmer, G.L., Barber, D., Andrews, J., 2003. Provenance of late quaternary ice-proximal sediments in the North Atlantic: Nd, Sr and Pb isotopic evidence. Earth Planet. Sci. Lett. 209, 227–243.
Frank, C., Terhorst, B., Damm, B., Thiel, C., Frechen, M., Peticzka, R., 2011. Pleistocene loess deposits and mollusc assemblages in the eastern Pre-Alps. E&G Quat. Sci. J. 60, 126–136.
Frechen, M., Boenigk, W., Weidenfeller, M., 1995. Chronostratigraphie des 'Eiszeitlichen Lossprofils' in Koblenz-Metternich. Mainzer Geowiss. Mitt. 24, 155–180.
Gallet, S., Jahn, B., Torii, M., 1996. Geochemical characterization of the Luochuan loess-paleosol sequence, China, and paleoclimatic implications. Chem. Geol. 133 (1–4), 67–88.
Gild, C., Geitner, C., Sanders, D., 2018. Discovery of a landscape-wide drape of lateglacial aeolian silt in the western Northern Calcareous Alps (Austria): first results

and implications. Geomorphology 301, 39–52. https://doi.org/10.1016/J.GEOMORPH. 2017.10.025.
Haase, D, Fink, J, Haase, G, Ruske, P, Pescsi, M, Richter, H, Altermann, M, Jager, K.D., 2007. Loess in Europe—Its spatial distribution based on a European Loess Map, scale 1:2,500,000. Quat. Sci. Rev. 26 (9), 1301–1312. https://doi.org/10.1016/j.quascirev.2007.02.003.
Hall, A.M., Migoń, P., 2010. The first stages of erosion by ice sheets: evidence from central Europe. Geomorphology 123, 349–363.
Hardt, J., Luthgens, C., Hebenstreit, R., Bose, M., 2016. Geochronological OSL: and geomorphological investigations at the presumed Frankfurt ice marginal position in northeast Germany. Quat. Sci. Rev. 154, 85–99.
Huber, J., 2014. Hangsedimente und Saprolithe als grundlegende Bestandteile der Critical Zone – Beispiele aus dem Bayerischen Wald und der Colorado Front Range. PhD- Thesis, Munich.
Huntley, D.J., Lamothe, M., 2001. Ubiquity of anomalous fading in K- feldspars and the measurment and correction for it in optical dat- ing. Can. J. Earth Sci. 38 (7), 1039–1106.
Hülle, D., Hilgers, A., Kühn, P., Radtke, U., 2009. The potential of optically stimulated luminescence for dating periglacial slope deposits – a case study from the Taunus area, Germany. Geomorphology 109, 66–78.
IUSS Working Group WRB, 2015. World Reference Base for Soil Resources 2014, update 2015 International Soil Classification System for Naming Soils and Creating Legends for Soil Maps. World Soil Resources Reports No. 106. FAO, Rome.
Jacobs, P.M., Mason, J.A., Hanson, P.R., 2012. Loess mantle spatial variability and soil horizonation, southern Wisconsin, USA. Quat. Int. 265, 43–53.
Jacobs, P.M., Mason, J.A., Hanson, P.R., 2011. Mississippi Valley regional source of loess on the southern Green Bay Lobe land surface. Wisconsin. Quaternary Res. 75 (3), 574–583.
Jahn, A., 1950. Less, jego pochodzenie i związek z klimatem epoki lodowej. Acta Geol. Pol., I, 3, 257–310. (in Polish).
Jary, Z., 1999. Ostatni cykl lesowy w Polsce SW. In: Jary, Z. (Ed.), III Seminarium Lessowe – Geneza i wiek pokrywowych utworów pylastych południowo-zachodniej Polski. Uniwersytet Wrocławski, Wrocław-Bożków, Poland, pp. 35–36.
Jary, Z., 1996. Chronostratygrafia oraz warunki sedymentacji lessów południowo - zachodniej Polski na przykładzie Płaskowyżu Głubczyckiego i Wzgórz Trzebnickich (Chronostratigraphy and the course of loess sedimentation in SW Poland on the example of the Głubczyce Upland and Trzebnica Hills). Acta Univ. Wratislaviensis 1766, Stud. Geograficzne 63, 103.
Jary, Z., Kida, J., 2000. Loess particles sources, transport and deposition on the example of SW Poland. Acta Univ.Wratislaviensis, Studia Geograficzne LXXIV, 71–77.
Jary, Z., Kida, J., Ciszek, D., 2001. Odsłonięcie lessów w Księginicach Małych (Masyw Ślęży). W: Jary, Z., Kida, J., (red), Osady plejstoceńskie przedpola Sudetów. XI Seminarium "Korelacja stratygraficzna lessów i utworów lodowcowych Polski i Ukrainy", Wrocław-Jarnołtówek 23-28.IX.2001, Instytut Geograficzny Uniw. Wrocł., 35–40.
Jary, Z., Ciszek D., 2004. Odsłonięcie lessów w Zaprężynie na Wzgórzach Trzebnickich. W: Jary, Z., (ed.), Zmiany klimatu zapisane w sekwencjach lessowych. IV Seminarium Lessowe, Strzelin 13-16 października 2004, Instytut Geografii i Rozwoju Regionalnego Uniwersytetu Wrocławskiego, 108–112.
Jary, Z., Ciszek, D., Kida, J., 2004. Odsłonięcie lessów w Białym Kościele koło Strzelina. W: Jary, Z., (red.), Zmiany klimatu zapisane w sekwencjach lessowych. IV Seminarium Lessowe, Strzelin 13-16 października 2004, Instytut Geografii i Rozwoju Regionalnego Uniwersytetu Wrocławskiego, 97–101.
Jary, Z., 2007. Record of Climate Changes in Upper Pleistocene loess-soil sequences in Poland and western part of Ukraine. Rozprawy Naukowe Instytutu Geografii i Rozwoju Regionalnego Uniwersytetu Wrocławskiego 1. Wrocław. (in Polish with English summary).
Jary, Z., 2009. Periglacial markers within the late pleistocene loess-palaeosol sequences in Poland and western part of Ukraine. Quat. Int. 198, 124–135.
Jary, Z., 2010. Loess–soil sequences as a source of climatic proxies: an example from SW Poland. Geologija 52, 40–45.
Johansson, Å., Waight, T., Andersen, T., Simonsen, S.L., 2016. Geochemistry and petrogenesis of Mesoproterozoic A-type granitoids from the Danish island of Bornholm, southern Fennoscandia. Lithos 244, 94–108. https://doi.org/10.1016/j.lithos.2015.11.031.
Kabała, C., Przybył, A., Krupski, M., Łabaz, B., Waroszewski, J., 2019. Origin, age and transformation of Chernozems in northern Central Europe – new data from Neolithic earthen barrows in SW Poland. Catena 180, 83–102.
Kabala, C., Bekier, J., Bińczycki, T., Bogacz, A., Bojko, O., Cuske, M., Ćwieląg-Piasecka, I., Dębicka, M., Gałka, B., Gersztyn, L., Glina, B., Jamroz, E., Jezierski, P., Karczewska, A., Kaszubkiewicz, J., Kawałko, D., Kierczak, J., Kocowicz, A., Krupski, M., Kusza, G., Łabaz, B., Marzec, M., Medyńska-Juraszek, A., Musztyfaga, E., Perlak, Z., Pędziwiatr, A., Pora, E., Przybył, A., Strączyńska, S., Szopka, K., Tyszka, R., Waroszewski, J., Weber, J., Woźniczka, P., 2015. Soils of lower silesia: origins, diversity and protection. PTG. PTSH, Wrocław pp. 256.
Kida, J., Jary, Z., 2004. Lessy Pogórza Kaczawskiego. Przyroda Sudetów Zachodnich, t. VI, 2003, 211–222.
Kleber, A., Terhorst, B., 2013. Mid-latitude slope deposits (cover beds) developments in sedimentology. Elsevier 66, 302.
Kleber, A., Dietze, M., Terhorst, B., 2013. Sedimentary properties of layers. In: Kleber, A., Terhorst, B. (Eds.), Mid-latitude slope deposits (Cover-Beds). Developments in Sedimentology 66 Elsevier, pp. 12–18.
Konieczna, N., Belka, Z., Dopieralska, J., 2015. Nd and Sr isotopic evidence for provenance of clastic material of the Upper Triassic rocks of Silesia, Poland. Ann. Soc. Geol. Pol. 85, 675–684.
Kowalska, J.B., Skiba, M., Maj-Szeliga, K., Mazurek, R., Zalewski, T., 2020. Does calcium carbonate influence clay mineral transformation in soils developed from slope deposits in Southern Poland? J. Soils Sediments. https://doi.org/10.1007/s11368-020-02764-3.
Kretz, R., 1983. Symbols for rock-forming minerals. Am. Mineral. 68, 277–279.
Lange, U., Bröcker, M., Armstrong, R., Żelaźniewicz, A., Trapp, E., Mezger, K., 2005a. The orthogneisses of the Orlica-Śnieżnik complex (West Sudetes, Poland): geochemical characteristics, the importance of pre-Variscan migmatization and constraints on the cooling history. J. Geol. Soc. 162, 973–984.
Labaz, B., Musztyfaga, E., Waroszewski, J., Bogacz, A., Jezierski, P., Kabala, C., 2018. Landscape-related transformation and differentiation of Chernozems — catenary approach in the Silesian Lowland. SW Poland. Catena 161. https://doi.org/10.1016/j.catena.2017.10.003.
Labaz, B., Kabala, C., Waroszewski, J., 2019. Ambient geochemical baselines for trace elements in Chernozems—approximation of geochemical soil transformation in an agricultural area. Environ. Monit. Assess. 191, 19.
Kryza, R., Pin, C., 2010. The Central-Sudetic ophiolites (SW Poland): Petrogenetic issues, geochronology and palaeotectonic implications. Gondwana Res. 17 (2–3), 292–305. https://doi.org/10.1016/j.gr.2009.11.001.
Labaz, B., Kabala, C., 2014. Origin, properties and classification of black earths in Poland. Soil Sci. Annu. 65 (2), 80–90.
Lange, U., Bröcker, M., Armstrong, R., Żelaźniewicz, A., Trapp, E., Mezger, K., 2005b. The gneisses of the Orlica-Śnieżnik complex (West Sudetes, Poland): geochemical characteristics, the importance of pre-Variscan migmatisation and constraints on the cooling history. J. Geol. Soc. London 162, 973–984.
Lin, Y.C., Feng, J.L., 2015. Aeolian dust contribution to the formation of alpine soils at Amdo (Northern Tibetan Plateau). Geoderma 259–260, 104–115.
Loba, A., Sykuła, M., Kierczak, J., Łabaz, B., Bogacz, A., Waroszewski, J., 2020. In situ weathering of rocks or an eolian silt deposition: key parameters for veryfing parent material and pedogenesis in the Opawskie Mountains - a case study from SW Poland. J. Soils Sediments 20, 435–451.
Lorz, C., Frühauf, M., Mail.nder, R., Phillips, J.D., Kleber, A., 2013. Influence of cover beds on soils. In: Kleber, A., Terhorst, B. (Eds.), Mid-Latitude Slope Deposits (Cover-Beds). Developments in Sedimentology. 66. pp. 95–125.
Luehmann, M.D., Peter, B., Connallon, C.B., Schaetzl, R.J., Smidt, S.J., Liu, W., Kincare, K., Walkowiak, T.A., Thorlund, E., Holler, M.S., 2016. Loamy, two-storied soils on the outwash plains of southwestern Lower Michigan: Pedoturbation of loess with the underlying sand. Ann. Assoc. Am. Geog. 106, 551–571.
Luehmann, M.D., Schaetzl, R.J., Miller, B.A., Bigsby, M.E., 2013. Thin, pedoturbated, and locally sourced loess in the western Upper Peninsula of Michigan. Aeolian Res. 8, 85–100.
Machalett, B., Oches, E.A., Frechen, M., Zöller, L., Hambach, U., Mavlyanova, N.G., Marković, S.B., Endlicher, W., 2008. Aeolian dust dynamics in central Asia during the Pleistocene: Driven by the long-term migration, seasonality, and permanency of the Asiatic polar front. Geochem. Geophys. Geosyst. 9, Q08Q09. https://doi.org/10.1029/2007GC001938.
Machalett, B., Frechen, M., Hambach, U., Oches, E.A., Zöller, L., Marković, S.B., 2006. The loess sequence from Remisowka (northern boundary of the Tien Shan Mountains, Kazakhstan) - Part I: Luminescence dating. Quat. Int. 152–153, 192–201.
Mange, M.A., Maurer, H.F.W., 1992. Heavy Minerals in Colour. Chapman and Hall, London, pp. 147.
Marcinkowski, B., Mycielska-Dowigałło, E., 2013. Heavy-mineral analysis in polish investigations of quaternary deposits: a review. Geologos 19, 5–23.
Marković, S.B., Bokhorst, M.P., Vandenberghe, J., McCoy, W.D., Oches, E.A., Hambach, U., Gaudenyi, T., Jovanović, M., Stevens, T., Zöller, L., Machalett, B., 2008. Late Pleistocene loess–palaeosol sequences in the Vojvodina region, North Serbia. J. Quat. Sci. 23, 73–84.
Marks, L., 2011. Quaternary Glaciations in Poland. In Ehlers, J., Gibbard, P.L., Hughes, P. D. (Eds.), Quaternary glaciations — extent and chronology, a closer look. Developments in Quaternary Science Vol. 15. Elsevier, Amsterdam, pp. 299–303.
Martignier, L, Nussbaumer, M, Adatte, T, Gobat, J.M., Verrecchia, E.P., 2015. Assessment of a locally-sourced loess system in Europe: The Swiss Jura Mountains. Aeolian Res. 18, 11–21. https://doi.org/10.1016/j.aeolia.2015.05.003.
Miller, B.A., Schaetzl, R.J., 2011. Precision of soil particle size analysis using laser diffractometry. Soil Sci. Soc. Am. J. 76, 1719–1727.
Morton, A.C., Hallsworth, C.R., 1999. Processes controlling the composition of heavy mineral assemblages in sandstones. Sed. Geol. 124, 3–29.
Morrás, H., 1999. Geochemical differentiation of Quaternary sediments from the Pampean region based on soil phosphorus contents as detected in the early 20th century. Quat. Int. 62, 57–67.
Moska, P., Jary, Z., Adamiec, G., Bluszcz, A., 2019. Chronostratigraphy of a loess-palaeosol sequence in Biały KościółPoland using OSL and radiocarbon dating. Quaternary Int. 502, 4–17.
Muhs, D.R., Bettis III, E.A., Skipp, G.L., 2018. Geochemistry and mineralogy of late quaternary loess in the upper Mississippi River valley, USA: Provenance and correlation with Laurentide ice sheet history. Quat. Sci. Rev. 187, 235–269.
Muhs, D.R., Budahn, J.R., Skipp, G.L., McGeehin, J.P., 2016. Geochemical evidence for seasonal controls on the transportation of Holocene loess, Matanuska Valley, southern Alaska, USA. Aeolian Res. 21, 61–73.
Muhs, D.R., 2013. The geologic records of dust in the Quaternary. Aeolian Res. 9, 3–48.
Munroe, J.S., Attwood, E.C., O'Keefe, S.S., Quackenbush, P.J.M., 2015. Eolian deposition in the alpine zone of the Uinta Mountains, Utah, US. Catena 124, 119–129.
Oberc-Dziedzic, T., Pin, C., Kryza, R., 2005. Early Palaeozoic crustal melting in an extensional setting: petrological and Sm–Nd evidence from the Izera granite-gneisses, polish sudetes. Int. J. Earth Sci. (Geol. Rundsch) 94, 354–368. https://doi.org/10.1007/s00531-005-0507-y.

O'Brien, Patrick J., Kröner, Alfred, Jaeckel, Petra, Hegner, Ernst, Żelaźniewicz, Andrzej, Kryza, Ryszard, 1997. Petrological and Isotopic Studies on Palaeozoic High-pressure Granulites, Góry Sowie Mts, Polish Sudetes. J. Petrol. 38 (4), 433–456. https://doi.org/10.1093/petroj/38.4.433.

Pańczyk, M., Nawrocki, J., Bogucki, B.A., Gozhik, P., Łanczont, M., 2020. Possible sources and transport pathways of loess deposited in Poland and Ukraine from detrital zircon U-Pb age spectra. Aeolian Res. 45, 100598.

Pawlak, W., 2008. Atlas of Lower and Opole Silesia, 2nd ed. Wroclaw University, Wroclaw, Poland.

Peng, W., Wang, Z., Song, Y., Pfaff, K., Luo, Z., Nie, J., Chen, W., 2016. A comparison of heavy mineral assemblage between the loess and the Red Clay sequences on the Chinese loess Plateau. Aeolian Res. 21, 87–91.

Pietranik, A., Kierczak, J., Tyszka, R., Schulz, B., 2018. Understanding heterogeneity of a slag-derived weathered material: the role of automated SEM-EDS analyses. Minerals 8, 513.

Przybyło, A., Pietranik, A., Schulz, B., Breitkreuz, C., 2020. Towards identification of zircon populations in permo-carboniferous rhyolites of Central Europe: insight from automated SEM-mineral liberation analyses. Minerals 10, 308.

Pye, K., 1995. The nature, origin and accumulation of loess. Quat. Sci. Rev. 14 (7–8), 653–667.

Raczyk, J., Jary, Z., Korabiewski, B., 2015. Geochemical properties of the Late Pleistocene loess-soil sequence in Dankowic. Landform Anal. 29, 49–61.

Raczyk J., 2013. Właściwości geochemiczne późnoplejstoceńskich lessów Wzgórz Trzebnickich i Wzgórz Niemczańsko-Strzelińskich. Uniwersytet Wrocławski, Instytut Nauk o Ziemi i Kształtowania Środowiska. Wrocław. (PhD thesis in Polish).

Rutanen, H., Andersson, U.B., Väisänen, M., Johansson, Å., Fröjdö, S., Lahaye, Y., Eklund, O., 2011. 1.8 Ga magmatism in southern Finland: strongly enriched mantle and juvenile crustal sources in a post-collisional setting. Int. Geol. Rev. 53, 1622–1683.

Römer, W., Lehmkuhl, F., Sirocko, F., 2016. Late Pleistocene aeolian dust provenances and wind direction changes reconstructed by heavy mineral analysis of the sediments of the Dehner dry maar (Eifel, Germany). Global and Planetary Change 147, 25–39.

Schaetzl, R., Bettis, E., Crouvi, O., Fitzsimmons, K., Grimley, D., Hambach, U., Zech, R., 2018. Approaches and challenges to the study of loess—Introduction to the LoessFest Special Issue. Quaternary Res. 89 (3), 563–618. https://doi.org/10.1017/qua.2018.15.

Schaetzl, R.J., Attig, J.W., 2013. The loess cover of northeastern Wisconsin. Quaternary Res. 79, 199–214.

Schaetzl, R.J., Loope, W.L., 2008. Evidence for an eolian origin for the silt-enriched soil mantles on the glaciated uplands of eastern Upper Michigan, USA. Geomorphology 100, 285–295.

Schaetzl, R.J., Luehmann, M.D., 2013. Coarse-textured basal zones in thin loess deposits: products of sediment mixing and/or paleoenvironmental change? Geoderma 192, 277–285.

Schatz, A.K., Qi, Y., Siebel, W., Wu, J., Zöller, L., 2015. Tracking potential source areas of Central European loess:examples from Tokaj (HU), Nussloch (D) and Grub (AT). Open Geosci. 7, 678–720.

Schulte, P., Sprafke, T., Rodrigues, L., Fitzsimmons, K.E., 2018. Are fixed grain size ratios useful proxies for loess sedimentation dynamics? experiences from Remizovka. Kaz. Aeolian Res. 31, 131–140.

Seguinot, J., Ivy-Ochs, S., Jouvet, G., Huss, M., Funk, M., Preusser, F., 2018. Modelling last glacial cycle ice dynamics in the Alps. Cryosphere 12, 3265–3285. https://doi.org/10.5194/tc-12-3265-2018.

Skurzyński, J., Jary, Z., Kenis, P., Kubik, R., Moska, P., Raczyk, J., Seul, C., 2020. Geochemistry and mineralogy of the Late Pleistocene loess-palaeosol sequence in Złota (near Sandomierz, Poland): implications for weathering, sedimentary recycling and provenance. Geoderma 375, 114459.

Smalley, I.J., O'Hara-Dhand, K., Wint, J., Machalett, B., Jary, Z., Jefferson, I.F., 2009. Rivers and loess: the significance of long river transportation in the complex event-sequence approach to loess deposit formation. Quaternary Int. 198, 7–18.

Sprafke, T., Fitzsimmons, K., Grützner, C., Elliot, A., Marquer, L., Nigmatova, S., 2018. Reevaluation of Late Pleistocene loess profiles at Remizovka (Kazakhstan) indicates the significance of topography in evaluating terrestrial paleoclimate records. Quat. Res. 89 (3), 674–690. https://doi.org/10.1017/qua.2017.103.

Sprafke, T., 2016. Loss in Niederosterreich - Archiv quart.rer Klima- und Landschaftsver. nderungen. Würzburg University Press, Würzburg, p. 272.

Sprafke, T., Obreht, I., 2016. Loess: rock, sediment or soil—what is missing for its definition? Quaternary Int. 399, 198207.

Stanley, K.E., Schaetzl, R.J., 2011. Characteristics and paleoenvironmental significance of a thin, dual-sourced loess sheet, northcentral Wisconsin. Aeolian Res. 2, 241–251.

Stevens, T., Palk, C., Carter, A., Lu, H., Clift, P.D., 2010. Assessing the provenance of loess and desert sediments in northern China using U-Pb dating and morphology of de- trital zircons. Geol. Soc. Am. Bull. 122, 1331–1344.

Szczepankiewicz, S., 1969. Sediments and forms of the far extents of Scandinavian Glaciations in SW Poland. Geogr. Polon. 17.

Tuhý, M., Hrstka, T., Ettler, V., 2020. Automated mineralogy for quantification and partitioning of metal(loid)s in particulates from mining/smelting-polluted soils. Environ. Pollut. 266 (1), 115118.

Tütken, T., Eisenhauer, A., Wiegand, B., Hansen, B.T., 2002. Glacial–interglacial cycles in Sr and Nd isotopic composition of Arctic marine sediments triggered by the Svalbard/Barents Sea ice sheet. Mar. Geol. 182 (3–4), 351–372.

Újvári, G., Klötzli, U., 2015. U-Pb ages and Hf isotopic composition of zircons in Austrian last glacial loess: constraints on heavy mineral sources and sediment transport pathways. Int. J. Earth Sci. 104, 1365–1385.

Újvári, G, Kok, J.F., Varga, G, Kovács, J, 2016a. The physics of wind-blown loess: Implications for grain size proxy interpretations in Quaternary paleoclimate studies. Earth Sci. Rev. 154, 247–278.

Újvári, G., Varga, A., Ramos, F.C., Kovács, J., Német, T., Stevens, T., 2016b. Evaluating the use of clay mineralogy, Sr–Nd isotopes and zircon U-Pb ages in tracking dust provenance: an example from loess of the Carpathian Basin. Chem. Geol. 304–305, 83–96.

Walczak, A., Belka, Z., 2017. Fingerprinting gondwana versus Baltica provenance: Nd and Sr isotopes in lower paleozoic clastic rocks of the małopolska and łysogóry terranes, southern Poland. Gondwana Res. 45, 138–151. https://doi.org/10.1016/j.gr.2017.02.002.

Waroszewski, J., Sprafke, T., Kabala, C., Musztyfaga, E., Labaz, B., Wozniczka, P., 2018a. Aeolian silt contribution to soils on the mountain slopes (Mt. Ślęża, SW Poland). Quat. Res. 89 (3), 702–717.

Waroszewski, J., Egli, M., Brandov, D., Christl, M., Kabala, C., Malkiewicz, M., Kierczak, J., Glina, B., Jezierski, P., 2018b. Identifying slope processes over time and their imprint in soils of medium-high mountains of Central Europe (the Karkonosze Mountains, Poland). Earth Surf. Process. Landf. 43 (6), 1195–1212.

Waroszewski, J., Sprafke, T., Kabala, C., Kobierski, M., Kierczak, J., Musztyfaga, E., Łabaz, B., 2019. Tracking textural, mineralogical and geochemical signatures in soils developed from basalt-derived materials covered with loess sediments (SW Poland). Geoderma 337, 983–997.

Waroszewski J., Sprafke T., Kabała C., Musztyfaga E., Kot, A., Tsukamoto S., Frechen M., 2020. Chronostratigraphy of silt-dominated Pleistocene periglacial slope deposits on Mt. Ślęża (SW, Poland): Palaeoenvironmental and pedogenic significance Catena 190 (2020) 104549 https://doi.org/10.1016/j.catena.2020.104549.

Weckwerth, P., Chabowski, M., 2013. Heavy minerals as a tool to reconstruct river activity during the Weichselian glaciation (Toruń Basin, Poland). Geologos 19, 25–46.

Wintle, A.G., 1973. Anomalous fading of thermoluminescence in mineral samples. Nature 245, 143–144.

Wolf, D., Ryborz, K., Kolb, T., Calvo Zapata, R., Sanchez Vizcaino, J., Zöller, L., Faust, D., 2019. Origins and genesis of loess deposits in central Spain, as indicated by heavy mineral compositions and grain-size variability. Sedimentology 66 (3), 1139–1161.

Valbracht, P.J., Oen, I.S., Beunk, F.F., 1994. Sm-Nd isotope systematics of 1.9-1.8-Ga granites from western Bergslagen, Sweden: inferences on a 2.1-2.0-Ga crustal precursor. Chem. Geol. 112 (1–2), 21–37.

Van Loon, A.J., 2006. Lost loesses. Earth-Sci. Rev. 74, 309–316.

Veit, H., et al., 2017. Late glacial/early holocene slope deposits on the swiss plateau: genesis and palaeo-environment. Catena 158, 102–112.

Völkel, J., Mahr, A., 1997. Neue Befunde zum Alter der periglazialen Deckschichten im Vorderen Bayerischen Wald. Z. Geomorphol. N. F. 41, 112–121.

Yaalon, D.H., Ganor, E., 1973. The influence of dust on soils during the quaternary. Soil Sci. 116, 146–155.

Yang, F., Karius, V., Sauer, D., 2020. Quantification of loess proportions in Pleistocene periglacial slope deposits and Holocene colluvium using grain-size data by laser diffractometry. J. Plant Nutr. Soil Sci. 183, 277–281.

Yates, K., Fenton, C.H., Bell, D.H., 2018. A review of the geotechnical characteristics of loess and loess-derived soils from Canterbury, South Island, New Zealand. Eng. Geol. 236, 11–21.

Zárate, M., 2003. The loess record of Southern South America. Quaternary Sci. Rev. 22, 1987–2006.

Zárate, M.A., Kemp, R.A., Blasi, A.M., 2002. Identification and differentiation of Pleistocene paleosols in the northern pampas of Buenos Aires, Argentina. J. South Am. Earth Sci. 15, 303–313.

Zárate, M.A., Tripaldi, A., 2012. The aeolian system of central Argentina. Aeolian Res. 3, 401–417.

Zerboni, A., Trombino, L., Frigerio, C., Livio, F., Berlusconi, A., Michetti, A.M., Rodnight, H., Spotl, C., 2014. The loess-paleosol sequence at Monte Netto: a record of climate change in the Upper Pleistocene of central Po Plain, northern Italy. J. Soils Sediments 15, 1329–1350. https://doi.org/10.1007/s11368-014-0932-2.

Zieliński, T., 2018. Prospects and limitations of heavy mineral analyses to discriminate preglacial/glacial transitions in Pleistocene sedimentary successions. Geologos 24 (2), 151–162.